Engineering Culture Platforms to Study Human Liver Cancer and Fibrosis

BY

Jennifer S. Liu
B.S., Fu Jen Catholic University, Taipei, Taiwan, 2011

THESIS

Submitted as partial fulfillment of the requirements
for the degree of Master of Science in Bioengineering
in the Graduate College of the
University of Illinois at Chicago, 2018

Chicago, Illinois

Defense Committee:

Salman Khetani, Chair and Advisor
David Eddington
James Lee

This thesis is dedicated to my parents, William Liu and Sue-Chi Lee, and my brother, John Liu, without their support and love I would never finish my master degree.

ACKNOWLEDGMENTS

I would like to first thank my advisor, Dr. Salman Khetani, for his guidance and support in my whole study. I would also like to thank my thesis committee members- Dr. David Eddington and Dr. James Lee, for their support and assistance to accomplish my thesis.

I would like to thank everyone in the lab, Brenton Ware, Chase Monckton, Christine Lin, David Kukla, Grace Brown, Regeant Panday, and Yang Yuan, for their assistance and help of my study.

TABLE OF CONTENTS

TABLE OF CONTENTS (continued)

LIST OF FIGURES

LIST OF FIGURES (continued)

LIST OF ABBREVIATIONS

ANOVA	Analysis of variance
ATP	Adenosine triphosphate
CDH1	E-cadherin
CDH2	N-cadherin
C-MPCC	Hepatocyte/cholangiocyte co-culture
C-MPTC	Hepatocyte/cholangiocyte/fibroblast tri-culture
CYP450	Cytochrome P450
DMEM	Dulbecco's Modified Eagle's Medium
DMEM/ F-12	Dulbecco's Modified Eagle's Medium/ F-12
DMF	Dimethyl formamide
DMSO	Dimethyl sulfoxide
ECM	Extracellular matrix
EGF	Epidermal growth factor
ELISA	Enzyme-linked immunosorbent assay
EMT	Epithelial-mesenchymal transition
HBV	Hepatitis B virus
HCC	Hepatocellular carcinoma
HCV	Hepatitis C virus
MET	Mesenchymal-epithelial transition
MPCC	Micropatterned co-culture
MPH	Micropatterned pure hepatocytes culture

LIST OF ABBREVIATIONS (continued)

NASH	Non-alcoholic steatohepatitis
PHH	Primary human hepatocyte
VEGFR	Vascular endothelial growth factor receptor
VIM	Vimentin

SUMMARY

The liver executes a plethora of functions such as drug metabolism, plasma protein secretion, and urea synthesis. Additionally, drug toxicity to the liver is a leading cause of drug attrition and liver cancer is the third leading cause of cancer-related deaths worldwide. Given differences between animals and humans in liver pathways, models of the human liver are essential for mechanistic studies and for drug screening. Unfortunately, human liver cells, both primary and cancer-derived, display low liver cell functions in conventional 2D monolayers. The micropatterned coculture (MPCC) platform, in which hepatocytes are organized onto collagen domains of empirically optimized dimensions and subsequently cocultured with fibroblasts, has been shown to induce high hepatocyte functions for several weeks. However, the current configuration of MPCCs lacks a key cell type of the liver, cholangiocytes (biliary epithelial cells), and it is not clear if MPCCs can be used for the development of a liver cancer screening system.

This thesis aims to address these abovementioned limitations. Results obtained demonstrate that several liver cancer cell lines cultured in the MPCC platform maintain cell proliferation, higher liver cell functions, and can be effectively used to determine cytotoxicity of cancer drugs and detect cancer related gene expression. Furthermore, results show that while cholangiocytes cannot support primary human hepatocytes to the same extent as the fibroblasts, creation of a three-cell type model (hepatocytes, cholangiocytes, and fibroblasts) with higher ratio of fibroblasts and lower ratio of cholangiocytes allows high levels of functions in hepatocytes and retention of cholangiocyte morphology. Interestingly, three-cell type model also showed significantly inhibition of hepatic function and displayed increased microvascular steatosis which

may suggest that the three-cell type model could be developed as a liver disease (e.g. fibrosis) model. In conclusion, the model systems developed are potentially useful for fundamental research in liver cancer and hepatocyte-cholangiocyte interactions, and for screening the cancer related pathways and efficacy and/or toxicity of drugs. In the future, the model systems can be integrated to study the effects of cholangiocytes in liver diseases or on liver cancer cells and to build models of both hepatocellular carcinoma and cholangiocarcinoma (liver cancer subtypes).

CHAPTER 1. HUMAN LIVER CANCER MODEL

1.1 INTRODUCTION

1.1.1 Background of liver cancer

Liver cancer is the second leading cause of cancer mortality in men and the sixth leading cause in women worldwide [1]. The incidence rates in U.S. increase about 3% to 4% per year and 5-year survival rate is lower than 20% [2]. Among primary liver cancer, about 70% to 85% of cases are hepatocellular carcinoma (HCC) which is the most common subtype of primary liver cancer [1]. The difficulty of curing liver cancer and high death rate may be caused by clinical and biological heterogeneity [3]; furthermore, the variability of HCC is likely due to many factors like body condition of patients, different diseases that lead to liver cancer such as hepatitis B virus (HBV), hepatitis C virus (HCV), alcohol-related cirrhosis, nonalcoholic fatty liver disease, and obesity. In addition, the heterogeneity of cancer also affects drug development. Since heterogeneity of HCC makes it difficult to find target genes and good therapies, the cost of drug development is huge every year. For a single successful drug, the highest estimated cost is about $2.7 billion [4]. Part of the cost may be due to the failed drugs in a therapeutic program. Many of the drugs fail in clinical tests which may suggest the need for a new strategy for pre-clinical testing [5, 6]. In this study, we focus on *in vitro* pre-clinical model which can maintain cell differentiation and hepatic functions of liver cancer cell lines. Moreover, this model can be used to investigate cancer or drug related gene expression as well as screen with cancer drugs.

1.1.2 Current liver models

The drug development process is divided into subcategories including drug discovery, pre-clinical tests, and clinical tests (**Figure 1**). Both *in vitro* and *in vivo* liver models were developed for drug screening in pre-clinical tests. The *in vivo* animal models are good to mimic cancer microenvironment and control the conditions of cancer. However, the cost of animal models is usually higher than *in vitro* models and the difference between animal and human cells may cause different drug effects [5, 7]. Additionally, ethical concerns have been raised regarding reliance on animal testing [8]. Based on the reasons above, increased number of *in vitro* models are used for drug screening. Two-dimensional (2D) conventional cell cultures are efficient and used for many years. However, hepatocytes lose functions and viability rapidly in 2D conventional mono-cultures [9]; therefore, some methods such as sandwich cultures, co-culture platforms, and three-dimensional (3D) cultures have been developed.

Human hepatocytes were cultured in collagen-Matrigel sandwich culture and used for short-term research [10]. Then, the micropatterned co-culture (MPCC), in which hepatocytes are patterned onto collagen islands and co-cultured with surrounding fibroblasts, has been shown to induce high hepatocyte functions for several weeks [11]. It has been used for many hepatotropic pathogen studies such as HBV and HCV [12] and various cell types that co-culture with primary hepatocytes such as hepatic stellate cells [13] and endothelial cells [14]. However, it is not clear if fibroblast can also stabilize liver cancer cell lines and if the MPCC platform can be used for liver cancer drug toxicity screening. Another type of models is 3D culture platforms which are used often in cancer research since 3D cultures can better mimic the natural microenvironment of tumors in human body. Porous alginate scaffold has been reported to create 3D organotypic liver cancer cells culture models [15] and hanging drop method has been used for 3D heterospheroid

models [16]. These 3D cultures that mimic 3D tumor environment were shown to provide extracellular matrix (ECM) barrier, maintain cell viability, and could be used for drug screening. However, the result of hepatic functions such as albumin secretion and cytochrome P450 (CYP450) activities is limited. Therefore, there is a need for a liver cancer model that can maintain cell differentiation and show hepatic functions such as CYP enzyme activities that may increase drug resistance of cancer cells as *in vivo*.

1.1.3 Purpose of the study

In this study, the purpose is to create a liver cancer cell *in vitro* model which can be used in pre-clinical testing for drug screening and investigating liver cancer and drug related genes. To develop liver cancer models, well differentiated hepatocellular carcinoma cell lines, HepG2, HepaRG, and Huh 7 (which are normally used for HCC research) were cultured within the MPCC platform. These models were evaluated by comparison of cell morphology and hepatic functions including albumin secretion, CYP enzyme activities and cancer related gene expressions. Based on the comparative analysis, the suitable models that maintained higher and stable hepatic functions were created and chosen for drug screening. To compare the effects of different drugs, selected models were treated with five liver cancer drugs. Albumin secretion and cell viability were measured to elucidate drug effects on the liver cancer models.

1.2 MATERIALS AND MATHODS

1.2.1 Micropatterned co-culture of liver cancer cell lines and fibroblast 3T3-J2

HepG2 cells were obtained from American Tissue Culture Collection (Manassas, VA). HepaRG cells were obtained from Biopredic International (France). Huh 7 cells were obtained from Charles Rice at Rockefeller University (New York, NY). HepG2 and Huh 7 vials were thawed in 37°C water bath for 120s and diluted in 25ml of hepatocyte seeding media (the formulation was described previously [17]). Then the cell suspension of HepG2 was spun at 500xg for 5min and Huh 7 cells was spun at 1000rpm for 5min. The supernatant was discarded and then the cells were re-suspended in hepatocyte seeding medium. HepaRG vials were thawed in 37°C water bath for 120s and diluted in 8ml of hepatocyte seeding media. Then the cell suspension without spinning was used for cell counting directly. Cancer cell viability was assessed by using the trypan blue exclusion method.

MPCCs were created as previous described [12] (**Figure 2**). Briefly, adsorbed rat tail collagen I was lithographically patterned in each well of a multi-well plate to create 500 μm diameter circular domains spaced 1200 μm apart, center-to-center. Liver cancer cells were seeded (~30K cells per well of a 96-well plate and ~180K cells per well of a 24-well plate) and selectively attached to the collagen domains on ~13 collagen-coated islands within each well of a 96-well plate and ~90 collagen-coated islands within each well of a 24-well plate. The next day, after cancer cells were spread to fill in the collagen islands, 3T3-J2 fibroblasts ,which were cultured and passaged as previous described [11], were seeded at ~15k cells per well in a 96-well

plate and ~90k cells per well in a 24-well plate. Micropatterned pure hepatocytes cultures (MPHs) were created by the same protocol above but without fibroblast seeding.

1.2.2 Quantitative polymerase chain reaction (qPCR)

RNA was extracted from 24-well plate cultures with the GeneJET RNA Purification Kit (Thermo Fisher Scientific, Waltham, MA) and homogenized by homogenizing columns (Omega Bio-Tek, Norcross, GA). RNA was treated with DNAse I (New England Biolabs, Ipswich, MA) to remove genomic DNA and reverse transcribed into complementary DNA (cDNA). Then, 250ng of cDNA was used in qPCR with the Taqman™ master mix (Thermo Fisher Scientific) and pre-designed Taqman human-specific primer/probe sets including E-cadherin (CDH1), N-cadherin (CDH2), and vimentin (VIM). All gene expression data was normalized to the data of GAPDH and then normalized to the data of first time point of MPH.

1.2.3 Quantification of cell functionality

Culture supernatants were collected every two days and assessed for albumin concentration using the protocol as previously described [11]. Briefly, albumin concentration was determined by using a competitive enzyme-linked immunosorbent assay (ELISA) with horseradish peroxidase detection and 3,3’,5,5’-tetramethylbenzidine (TMB, Rockland Immunochemicals, Boyertown, PA) as the substrate. CYP2A6 enzyme activity was measured by incubating the cultures with substrate, coumarin (Sigma-Aldrich, St. Louis, MO), for 1 hour at 37°C. Then the modification of coumarin to fluorescent 7-hydroxy-coumarin was detected to measure the CYP2A6 activity.

1.2.4 Drug dosing and cell viability

HepG2 MPCCs were cultured for 7 days and HepaRG MPCCs were cultured for 11 days to stabilize their functions. Fibroblast mono-cultures were cultured over the same time-period. Then MPCCs and fibroblast mono-cultures were dosed with drugs every two days for 6 days (3 total dosings) in 2% bovine serum supplement culture medium comprising of Dulbecco's Modified Eagle's Medium (DMEM, Corning), 2% of bovine serum (Life Technologies, Carlsbad, CA),15 mM HEPES buffer (Corning Cellgro, Manassas, VA), 1% vol/vol ITS+ supplement (Corning Life Sciences, Tewksbury, MA), 1% vol/vol penicillin-streptomycin (Corning Cellgro), and 100 nM glucagon (Sigma-Aldrich) with anti-cancer drugs. Sorafenib, 5-fluorouracil, doxorubicin, vincristine, and cisplatin were purchased from Cayman Chemical (Ann Arbor, Michigan, USA) and dissolved in dimethyl sulfoxide (DMSO, Corning) or dimethyl formamide (DMF, Sigma-Aldrich). The DMSO or DMF concentration that the cultures were exposed to was kept between 0.025% and 0.5% (vol/vol) relative to the culture medium for all drugs and control cultures were treated with DMSO or DMF at corresponding concentrations. Culture supernatants were collected for albumin assay as described above. Cell viability was measured every two days after drug dosing by using the PrestoBlue® cell viability reagent (Thermo Fisher Scientific) according to manufacturer's protocols.

1.2.5 Data analysis

Each experiment was carried out in triplicate wells for each condition. Microsoft Excel and GraphPad Prism (La Jolla, CA) were used for analyzing and graphing data. Error bars on graphs

represent standard deviation for each condition. Statistical significance was determined using two-way analysis of variance (ANOVA) with a Bonferroni test.

1.3 RESULTS

1.3.1 Morphology of liver cancer cell/fibroblast co-cultures and liver cancer cell mono-cultures

Liver cancer cell line HepG2, HepaRG, and Huh 7 could be patterned and HepG2 and HepaRG could form spheroids after two weeks in culture (**Figure 3**). For HepG2, the circular shape of the islands could be maintained but the islands became larger and spheroids of cancer cells were formed after two weeks (**Figure 3A and 3D**). In contrast, HepaRG cells were patterned after HepaRG seeding but the islands were infiltrated by the fibroblasts (**Figure 3B**); however, after two weeks, the HepaRG reorganized on the islands as spheroid-like cultures intermixed with the fibroblasts (**Figure 3E**). Unlike HepG2 and HepaRG, Huh 7 could maintain the micropatterned geometry for the first week (**Figure 3C**) but cells spread out and morphologically resembled monolayer cultures after two weeks (**Figure 3F**).

In comparison to the MPH controls, the MPCC format was found to help liver cancer cells form spheroids, likely due to the cell-cell heterotypic interactions introduced by the fibroblasts that inhibited cell spreading. In MPH controls, though HepG2 cells could maintain the pattern geometry for first week (**Figure 3G**), HepaRG and Huh 7 proliferated such that the island shapes became irregular and monolayers were established. (**Figure 3H and 3I**). After culturing for two weeks, HepG2 MPHs could form spheroids as in MPCCs; however, cell proliferation enlarged islands that caused islands to merge with each other and resemble conventional monolayer cultures; such results were similar to HepaRG and Huh7 cells after 1 week in culture (**Figure 3J**). Furthermore, HepaRG and Huh 7 did not display any evidence of spheroidal formation due to the transition into monolayers (**Figure 3K and 3L**).

1.3.2 Comparison of liver cancer cell/fibroblast co-cultures and liver cancer cell mono-cultures

To understand if MPCC platform can affect cancer related pathways in the cultured cancer cells, the gene expression of E-cadherin (a marker of epithelial cell), N-cadherin, and vimentin (markers of mesenchymal cell) were evaluated in MPCCs and MPH controls (**Figure 4**). These genes are the markers of epithelial-mesenchymal transition (EMT) pathway and mesenchymal-epithelial transition (MET) pathway which are known as important pathways of cancer development including HCC [18]. Overall, the results showed higher E-cadherin expression as compared to N-cadherin and vimentin expression. In addition, E-cadherin expression increased over three weeks. The results indicated that MPCC and MPH culture platforms could help liver cancer cells undergo MET pathway. For HepaRG cell line, E-cadherin expression of MPCCs is slightly higher than the expression of MPHs which suggested HepaRG cells in MPCCs underwent MET pathway more so than in MPHs; however, the results were not statistically significantly across MPCCs and MPHs.

At the functional level, to verify whether MPCCs maintain liver cell functions better than MPHs, albumin function and CYP enzyme activity were tested and MPHs were used as controls. For albumin function (**Figure 5A, 5C and 5E**), HepG2 and HepaRG in MPCCs demonstrated higher albumin function than MPH controls, with HepaRG displaying a greater differential. Moreover, the HepG2 and HepaRG in MPCCs maintained stable albumin secretion over three weeks. However, Huh7 in MPCCs showed similar albumin secretion levels as MPHs. For CYP enzyme activity (**Figure 5B, 5D, and 5F**), all three cell lines in MPCCs had higher CYP2A6 activities than in MPHs, especially for HepaRG co-cultures. CYP3A4 activities were also tested

and MPCCs could maintain enzymes activities but no significant different between MPCCs and MPHs were detected (data not shown). These data suggested that cell-cell interactions from fibroblasts support induction of most, if not all, drug metabolism pathways.

1.3.3 Cancer drug screening

As described above, Huh 7 could not form spheroids and maintain stable albumin secretion overtime. On the other hand, HepG2 and HepaRG in MPCCs could form spheroids and maintained increased liver functions than in MPHs. Therefore, the MPCC models of HepG2 and HepaRG were used in subsequent cancer drug screening studies. In general, culture medium without serum is used for drug screening to avoid drug binding to animal-derived serum proteins [19, 20]. However, the viability of the fibroblasts cultured in a serum-free culture medium (**Figure 6A**) decreased overtime. Fibroblast cells are a crucial cell type in MPCCs since the fibroblasts can support and stabilize liver cell functions as described above. Thus, to find a better media formulation that contained optimal serum levels for fibroblast maintenance with minimal drug binding, media titrated with various percentages of serum were tested prior to drug screening. Sorafenib, an FDA approved liver cancer drug, and HepG2 MPCCs were used to test serum and drug interaction. Fibroblast in serum-supplemented medium at 2%, 5%, and 10%, compared with a serum-free medium control, maintained viability for over three weeks in culture (**Figure 6A**). The drug toxicity data for sorafinib across the various media formulations suggested that higher serum levels caused the drug toxicity to decrease in cultures (**Figure 6B, C, and D**), potentially due to increased drug binding to higher concentrations of serum proteins. Both albumin function and cell viability of MPCCs increased with higher serum concentrations. However, similar results were observed when MPCCs were cultured in 2% serum supplemented

medium relative to the serum-free control. Thus, 2% serum supplemented medium was used for cancer drug screening in this study.

To understand toxicity of cancer drugs, albumin secretion and cell viability were measured in this experiment. Cell viability of fibroblast mono-cultures was measured as a control relative to the viability of liver cancer cells in MPCCs. It was also measured to know whether drugs can affect non-cancer cell type through cytotoxic, rather than hepatotoxic, pathways. Test 1 of fibroblast viability was done alongside HepG2s and the fibroblasts were cultured for 7 days before drug dosing. Test 2 of fibroblast viability was done alongside HepaRGs and the fibroblasts were cultured for 11 days. All cancer drugs tested here, sorafenib (**Figure 7**), 5-fluorouracil (**Figure 8**), doxorubicin (**Figure 9**), vincristine (**Figure 10**) and cisplatin (**Figure 11**), showed time-dependent hepatotoxicity based on albumin secretion data. In addition, temporal- and dose-dependent responses of toxicity were found. Interestingly, the results suggested that the various liver cancer-specific drugs caused different effects in the liver cancer cell model.

First, sorafenib (**Figure 7**) caused a decrease in cell viability for both MPCCs and fibroblasts. However, albumin function dramatically decreased which may indicate more toxicity to liver cancer cells. Unlike sorafenib, the toxicity of 5-fluorouracil (**Figure 8**) is lower for fibroblasts; moreover, the albumin function results indicated that 5-fluorouracil toxicity to liver cancer cells is lower and there is a delayed onset of toxicity. Doxorubicin caused toxicity to both liver cancer and non-cancer cells but higher toxicity was observed in fibroblasts (**Figure 9**). For vincristine (**Figure 10**), the viability results were similar to the results obtained with 5-fluorouracil. Specifically, viability of both MPCCs and fibroblast mono-cultures were similar

throughout the drug dosing period. However, without affecting cell viability, albumin function showed dramatic decrease over time which may suggest that vincristine caused high hepatotoxicity. The last drug tested was cisplatin (**Figure 11**), which also caused toxicity to both cell types but it affected albumin function more than cell viabilities.

1.4 DISCUSSION

In this study, we developed an *in vitro* liver cancer model for drug screening and investigating cancer related pathways. This model can be used to observe cell morphology easily using conventional microscopy (as opposed to confocal microscopy) and liver cancer cell lines could be stabilized and maintained hepatic functions in MPCC models via the inclusions of supporting fibroblasts. Additionally, gene expression could be detected and the results suggested that liver cancer cells in the MPCC models could undergo MET pathway and maintain cell differentiation for several weeks. Moreover, MPCCs could be used for drug screening. Co-culture of liver cancer cells and fibroblasts could show drug effect on cancer cell lines and non-cancer cell type. Drug effects of cell lines could be determined by detecting albumin secretion and cell viability. The results of drug effects showed that toxicity of liver cancer cells is time- and dose- dependent. Therefore, this model could support liver cancer cells long-term and is useful to investigate gene expression changes and the effects of cancer drugs on cells.

Three different liver cancer cell lines were used in this study. As the results showed above, the differences in morphologies and hepatic functions may be due to different origins of the liver cancer cell lines. HepG2 is a well differentiated human hepatocellular carcinoma cell line which was isolated from the hepatocellular carcinoma of a 15-year-old Caucasian American. This cell line is one of the most commonly used hepatoma cell lines in hepatotoxicity research [21, 22] and it shows epithelial morphology in culture. As we described above, HepG2 maintained higher E-cadherin expression and lower N-cadherin and vimentin expression which suggest that HepG2 may undergo MET pathway. MET pathway and EMT pathway are related to tumor formation and development [23, 24]. Cells undergoing EMT pathway lose cell-cell adhesion and increase

cell metastasis [25, 26]. In contrast, MET pathway has the opposite role as the EMT pathway. HepG2 underwent MET pathway and expressed epithelial features that maintained cell differentiation but decreased cell metastasis. Therefore, HepG2 could form spheroids in both MPCCs and MPHs. Although, HepG2 cultured in both MPCC and MPH culture platforms could show epithelial cell features and form spheroids. However, due to the support of fibroblasts, HepG2 in MPCCs performed higher hepatic functions than in MPHs.

Another hepatoma cell line, HepaRG, could also form spheroids and showed higher hepatic functions only when cultured in the MPCC culture platforms. HepaRG, which was derived from a hepatocellular carcinoma with HCV, is a bipotential progenitor cell type that can differentiate to hepatocyte-like and cholangiocyte-like cells [27, 28]. We found that increased hepatic functions may suggest that with the support of fibroblasts, HepaRG displayed more hepatocyte-like functions. Spheroid formation of HepaRG in MPCCs showed similar morphology to HepaRG clusters cultured with 2% dimethyl sulfoxide that can induce HepaRG differentiation toward hepatocyte-like cell type [28], which may also prove that HepaRG cultured in MPCCs showed more hepatocyte-like cell type. Therefore, comparing to HepaRG in MPHs, cells in MPCCs had higher hepatic functions and could form spheroids.

In contrast, Huh 7 showed very different results of both cell morphology and hepatic functions. Huh 7, a well differentiated hepatocellular carcinoma cell line, was isolated from a 57-year old Japanese male [29]. In our study, we observed that Huh 7 grew faster as compared to the other two liver cancer cell lines. Although fibroblasts were co-cultured with Huh 7 in MPCCs, fibroblasts could not be clearly observed over three weeks which may be due to Huh 7 overgrowing onto the fibroblasts. Rapid cell proliferation may be due to a hepatoma-derived

growth factor that is secreted by Huh 7 [30]. Therefore, unlike the other cell lines which may grow only due to the inclusion of serum in the culture medium, Huh7 may grow due to their own growth factor secretions as well as the presence of serum. We anticipate that further optimization of the serum concentration may be needed to obtain stably functional Huh7-based MPCCs.

Micropatterened co-culture was shown to improve CYP enzyme activities of primary human hepatocytes [11]. Here, liver cancer cell lines cultured in MPCCs maintained CYP enzyme activities. Although the activities are lower than the activities of primary human hepatocytes [31], it can support cancer cell lines to resist cancer drugs that are metabolized by CYP enzymes, as would likely be the case *in vivo* in patients suffering from HCC. As we described above, sorafeniib, doxorubicin and cisplatin showed similar trend of albumin secretion and cell viability. Sorafenib is an FDA approved drug for hepatocellular carcinoma that inhibits tyrosine and serine/threonine kinases including vascular endothelial growth factor receptor (VEGFR) and Raf [32-34]. The inhibition of these kinases causes a decrease of cell proliferation and angiogenesis of cancer cells and then causes cell apoptosis. Besides, since these kinases also relate to normal cell physiology [35-37], the inhibition of these kinases also inhibits non-tumor cell proliferation. Another drug, doxorubicin, is a multi-cancer drug that can inhibit topoisomerase II as well as generate reactive oxygen species which cause DNA damage, cell membrane damage, and apoptosis [38, 39]. Cisplatin is a drug that uses for multiple types of cancers which can interfere DNA replication and cause cell apoptosis [40]. Compared to the results of doxorubicin and sorafenib, cisplatin caused both tumor and non-tumor cell death; however, the fibroblasts were more resistant to cisplatin since the drug more strongly affects faster growing cells like cancer cells.

In contrast to the results discussed above with doxorubicin, sorafenib, and cisplatin, 5-fluorouracil and vincristine affected liver cancer cells more in this study. 5-fluorouracil is a cancer drug that inhibits thymidylate synthase, interferes with RNA synthesis, and causes DNA and RNA damage [41]. Thymidine phosphorylase is one of the important enzymes that converts 5-fluorouracil to active metabolites. The level of thymidine phosphorylase in a tumor is higher than in normal tissues [42-44]; therefore, the cancer cells in the tumor are more susceptible to 5-fluorouracil toxicity. In this study, we found that 5-fluorouracil caused more toxicity to liver cancer cell lines than fibroblasts which may be due to more active metabolites produced in the cancer cells. Another drug, vincristine, is an anti-cancer drug that inhibits microtubule polymerization which inhibits cell division and causes growth arrest of cells [45]. Based on the viability of MPCCs we described above, vincristine seemed to have no effect on the cell viability of both cell types but did cause a dramatic decrease in albumin secretion. It may suggest that vincristine affected albumin functions strongly. Clinical results have shown that vincristine may cause liver injury and abnormal hepatic functions [46]. Although the mechanism is not clear, it may support our finding that vincristine decreased albumin secretion.

Generally, tumors develop 3D structures in the human body. Liver cancer cells in 2D conventional culture may have altered gene expression, lack cell-cell interactions and cannot mimic the complex tumor microenvironment as well as maintain cell functions [9, 47-50]. Our models could maintain hepatic functions and form spheroids of liver cancer cell lines. However, cells could form just semi-spheroids and no 3D ECM supported the cells to form a 3D structure. The lack of 3D cell-cell and cell-ECM interactions may change morphology and physiology of cancer cells. Previous articles reported multiple methods of using 3D cultures and ECM

scaffolds. Hanging drop method [16, 51], decellularized scaffolds [52], and rotational wall vessel bioreactors [53] were used to form 3D structure of liver cancer cells for cancer research. For ECM, collagen and alginate were used to support cancer cell lines for 3D cultures [16, 54]. These 3D cultures have been proved to maintain cell functions and viability. In addition, to improve cell functions, co-cultured cell types that can support liver cancer cells also play a crucial role in 3D tumor models. In our study, 3T3-J2 fibroblasts were used to support liver cancer cells. However, 3T3-J2 is not a human cell type. The interaction between cancer cells and cancer associated stromal cells creates a complex tumor environment [55]. Hepatic stellate cells, endothelial cells, and macrophages have been reported to support tumor growth as well as cause angiogenesis and inflammation [56-59]. All these cell types may need to be considered for improving MPCC-based liver cancer models in the future.

In conclusion, we created an in vitro liver cancer model that supported hepatic functions and could be used for drug screening and gene expression analysis. To understand the role of drug metabolism in cancer cell MPCCs, CYP3A4 enzyme activity was inhibited using a small molecule drug; however, no significant difference was detectable between the cells treated with cancer drug and the cells treated with both cancer drug and inhibitor (data not show). Further experiments of drug metabolism pathways will need to be carried out in the future. In addition, to mimic tumor microenvironment, 3D cultures of liver cancer cell lines with ECM and other cancer related cell types such as hepatic stellate cells and macrophages may be considered to improve pathophysiological relevance of this liver cancer model.

FIGURES

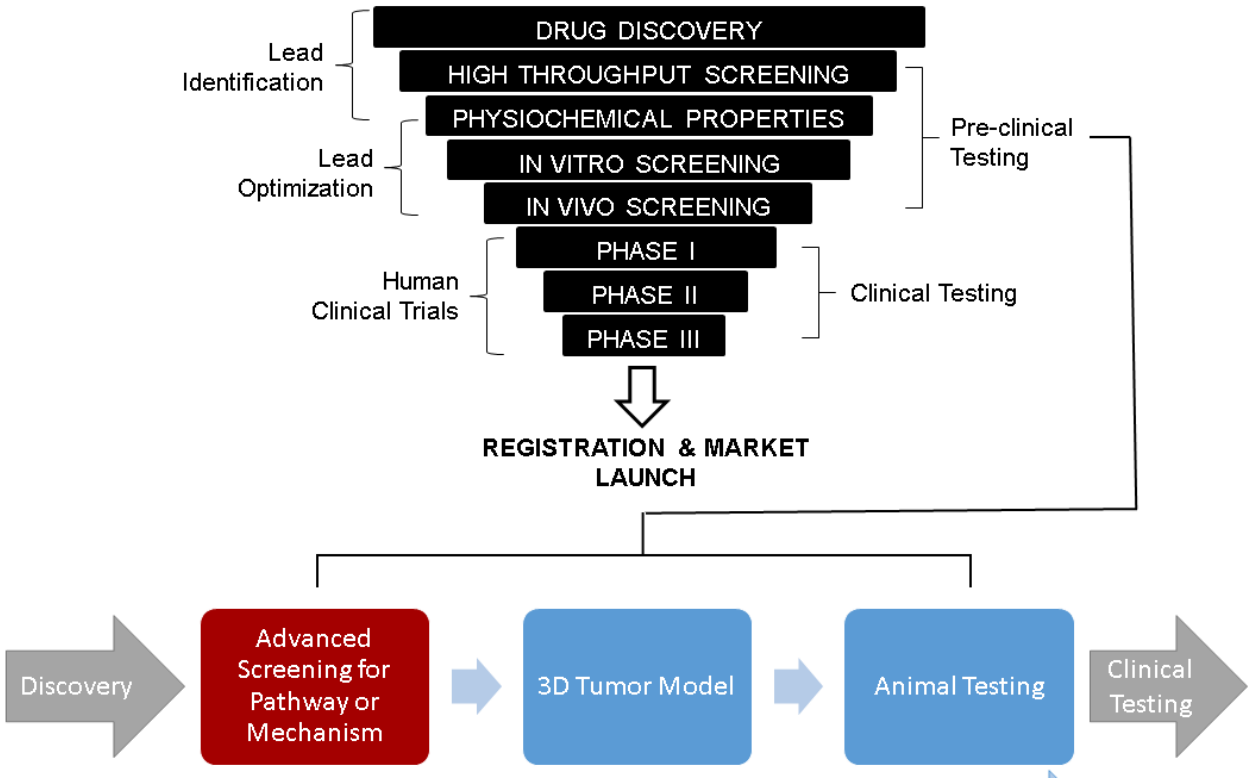

Figure 1. Drug development process (with permission of SAGE Publications)[60]. Here, we focused on the advanced screening for cancer and drug related pathway and mechanism (red square) in the pre-clinical testing process.

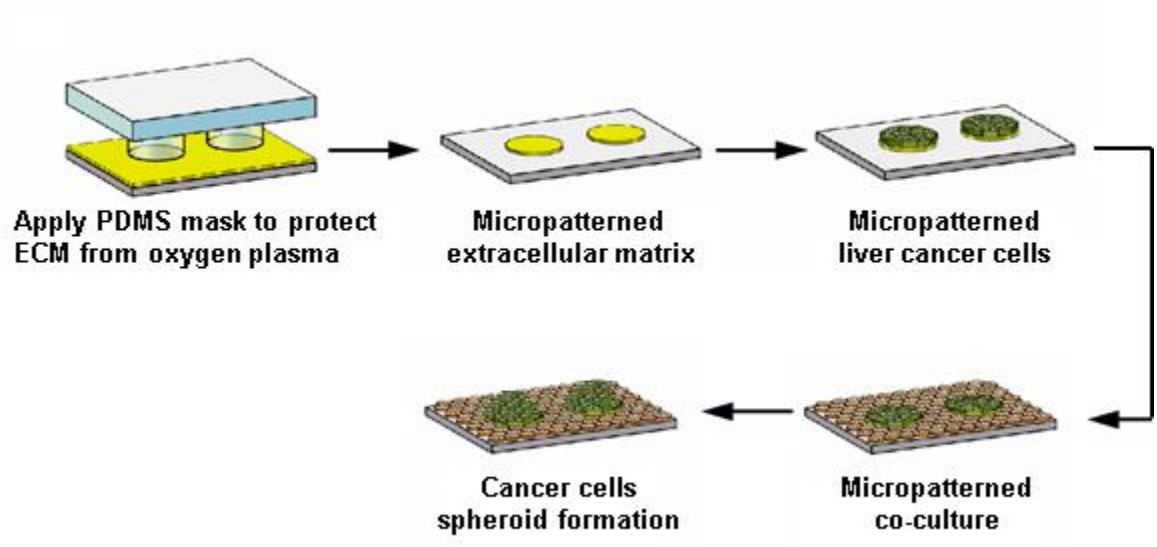

Figure 2. Process of micropatterned co-culture and spheroid formation of liver cancer cell lines (with permission of SAGE Publications)[60].

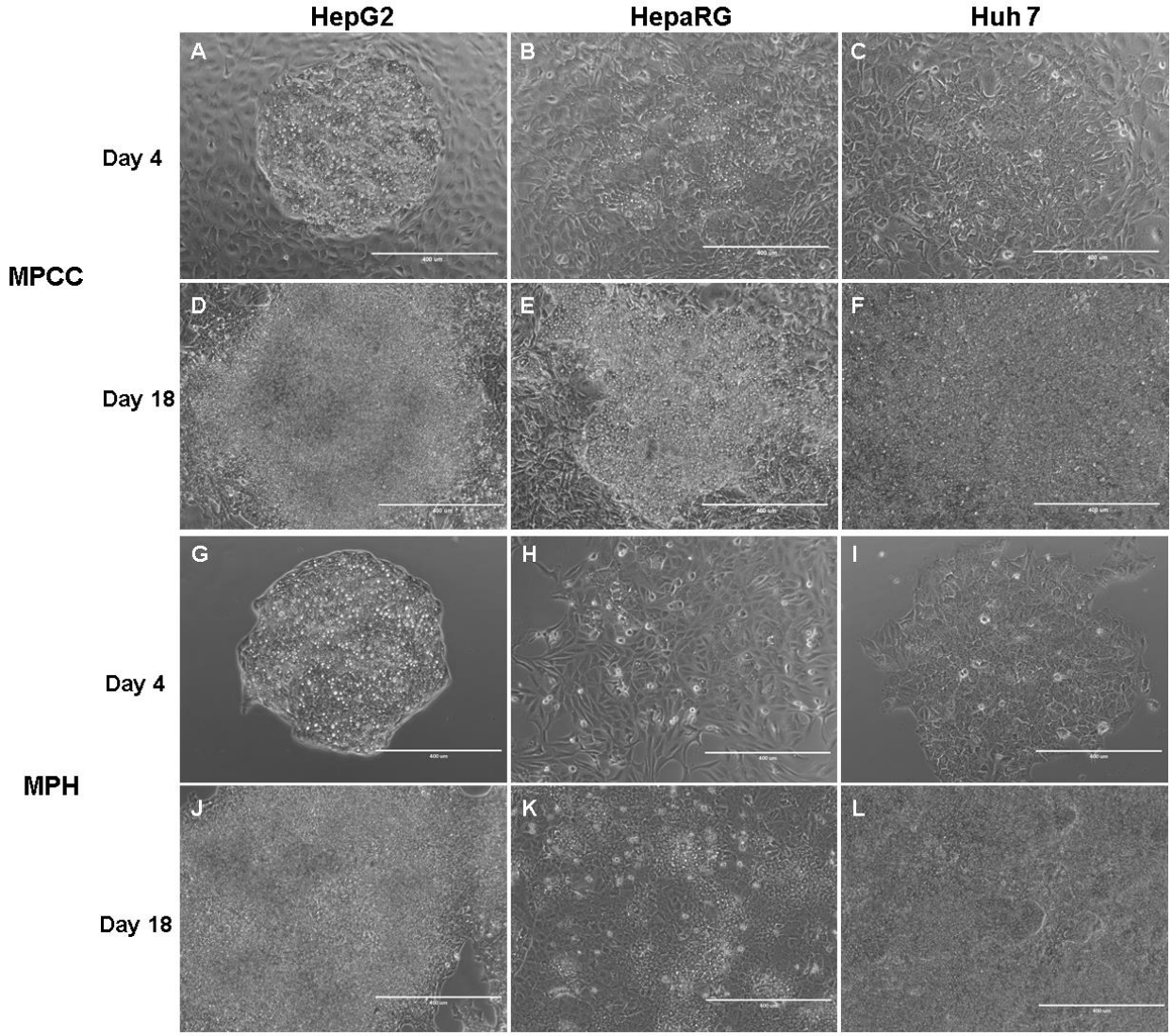

Figure 3. Morphology of liver cancer cell/fibroblast co-cultures (top) relative to patterned liver cancer cell mono-cultures (bottom). HepG2 and HepaRG MPCCs showed spheroid formation over 18 days but no spheroid formed in Huh 7 MPCC. In MPHs, HepG2 form spheroids over 18 days but HepaRG and Huh 7 cells spread and grew like in 2D monolayer cultures. All scale bars = 400 µm.

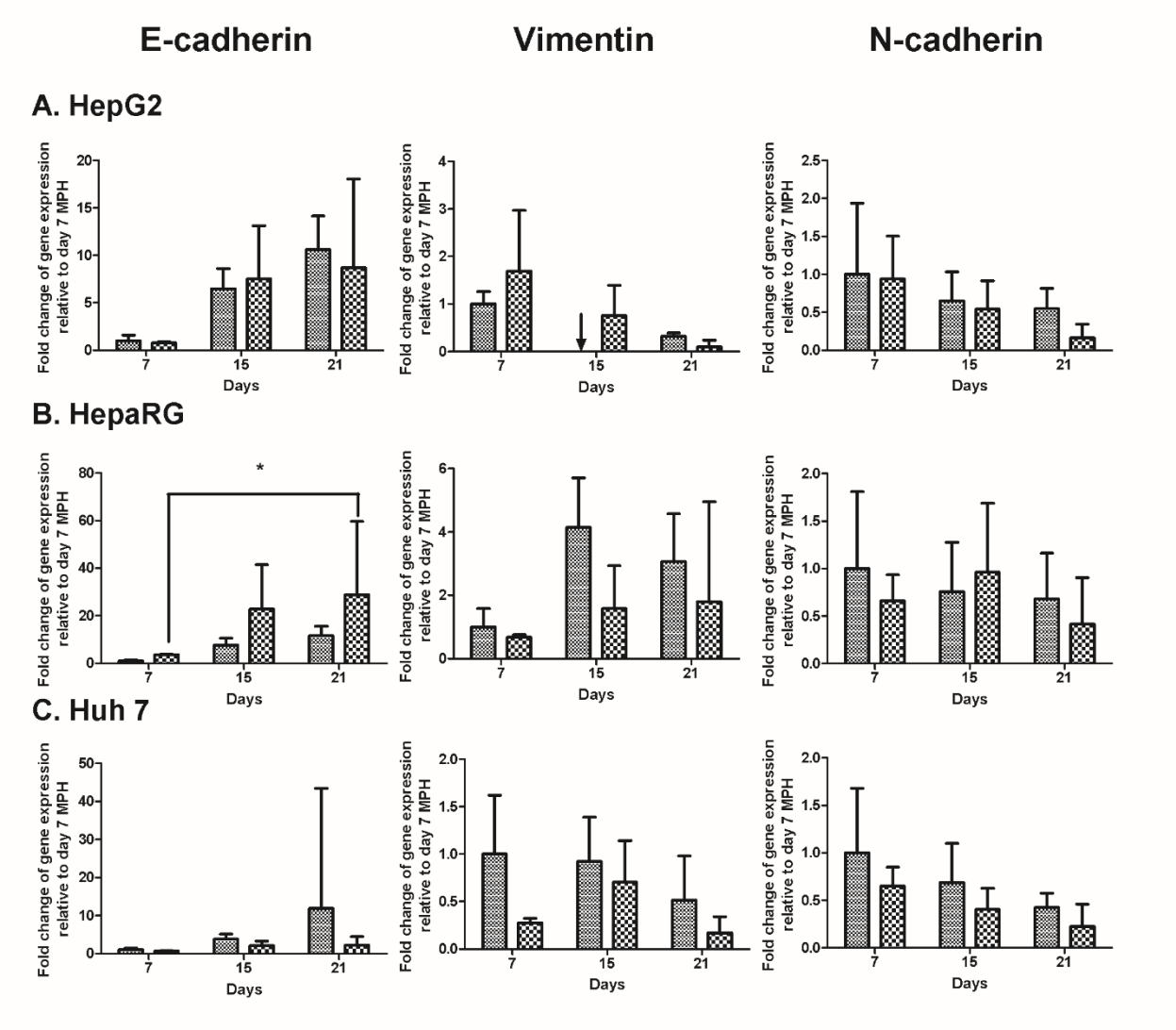

Figure 4. EMT and MET pathways related gene expressions. RNA was extracted from MPCC and MPH of HepG2 (A), HepaRG (B), and Huh 7 (C) to assess gene expression of E-cadherin vimentin, and N-cadherin. *$P < 0.05$

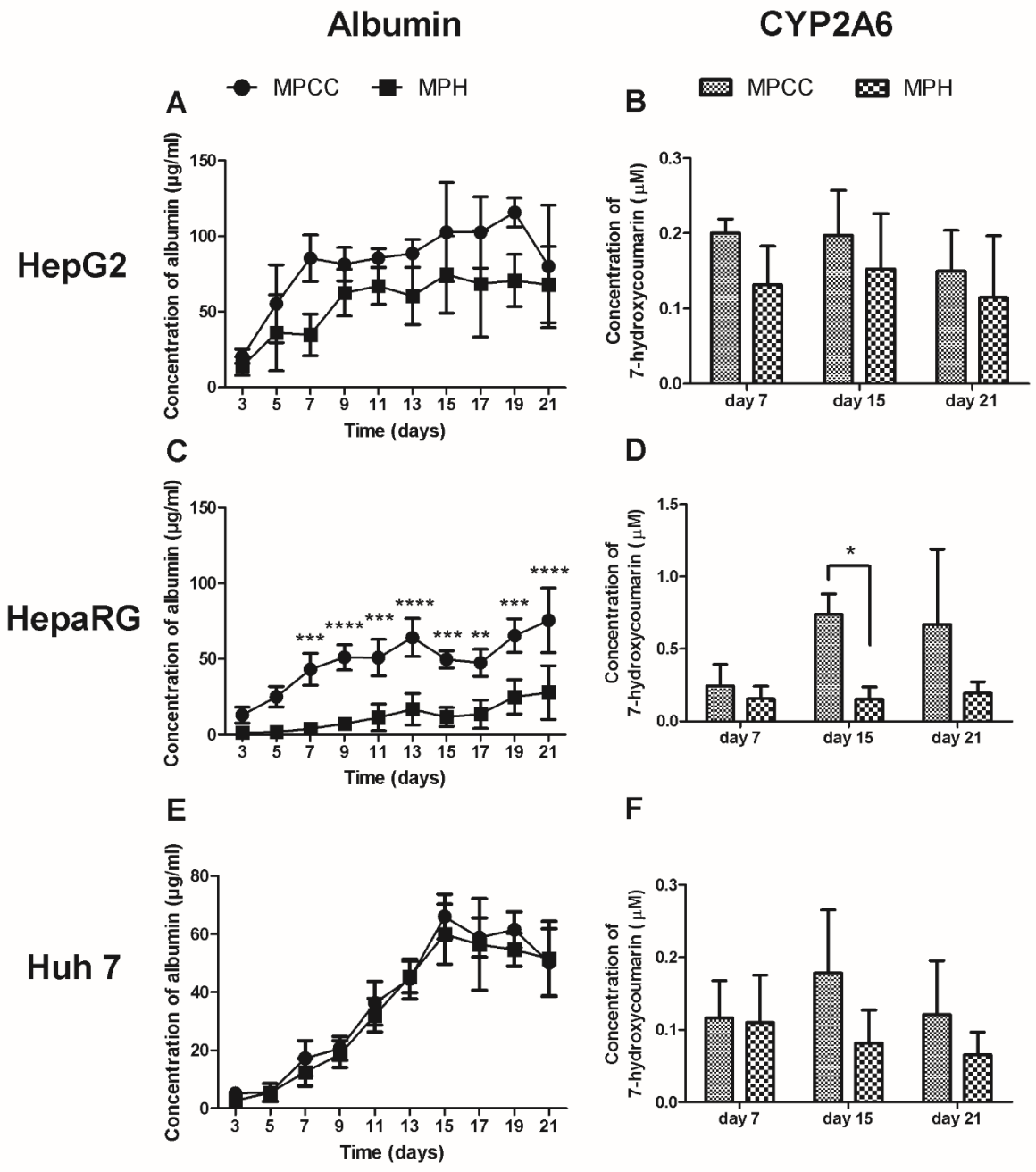

Figure 5. Functions of liver cancer models. Functions of MPCC models as compared to MPH models including albumin secretion (left) and CYP2A6 enzyme activity (right). *$P < 0.05$, **$P < 0.01$, ***$P < 0.001$, and ****$P < 0.0001$.

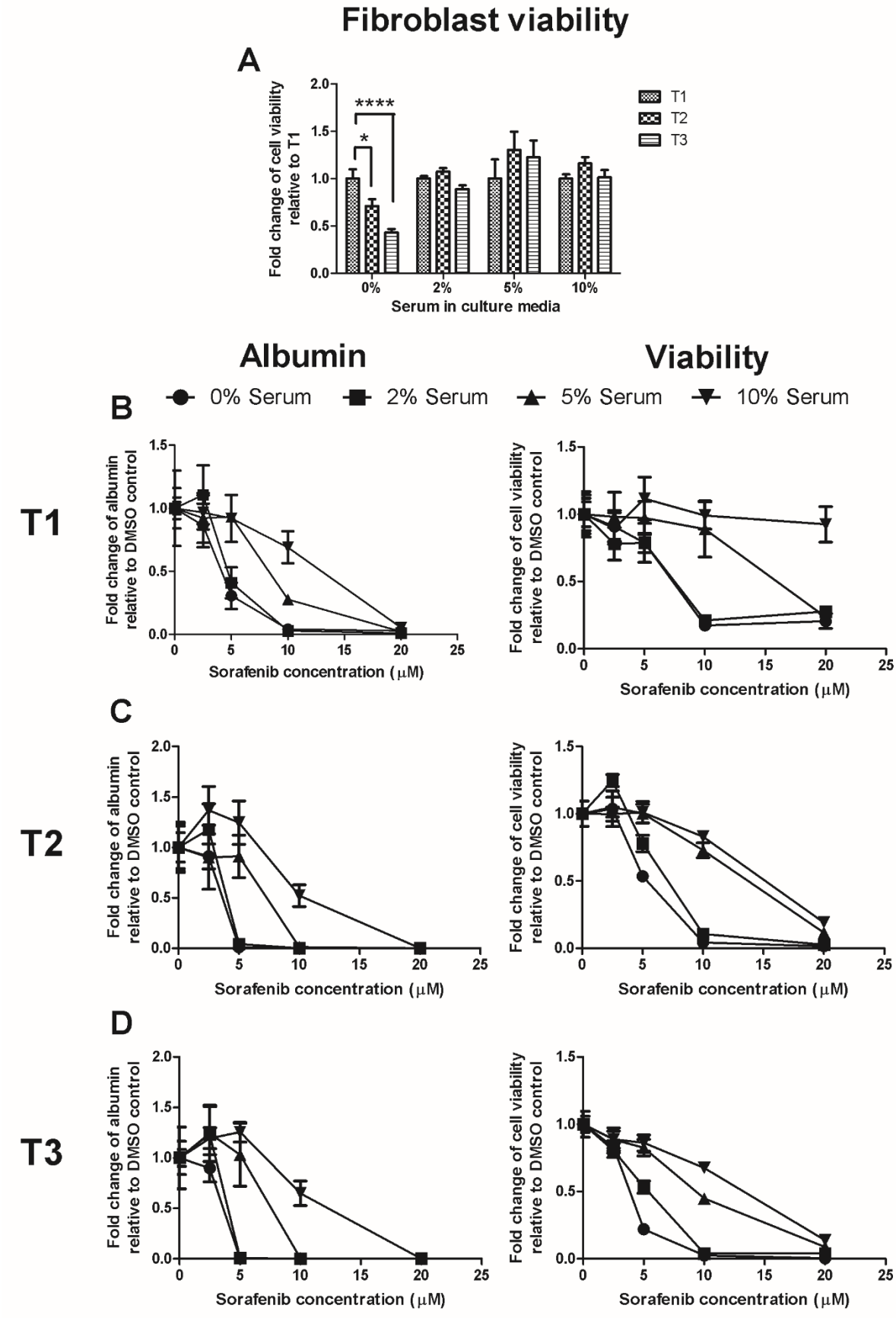
Fibroblast viability
A
Fold change of cell viability relative to T1
****
*
T1
T2
T3
0%
2%
5%
10%
Serum in culture media
Albumin
Viability
0% Serum
2% Serum
5% Serum
10% Serum
B
C
D
T1
T2
T3
Fold change of albumin relative to DMSO control
Fold change of cell viability relative to DMSO control
Sorafenib concentration (μM)

Figure 6. Serum test for drug-serum interactions. (A) Fibroblast viability in 0%, 2%, 5%, and 10% serum-supplemented medium containing DMSO. (B)-(D) Albumin secretion and cell viability at different time points in HepG2 MPCCs treated with drugs dissolved in media supplemented with varying concentrations of serum (or serum-free). Data is presented relative to the DMSO-treated control cultures. T1=2 days after treatment with drugs; T2=4 days after treatment with drugs; T3=6 days after treatment with drugs. *$P < 0.05$, and ****$P < 0.0001$.

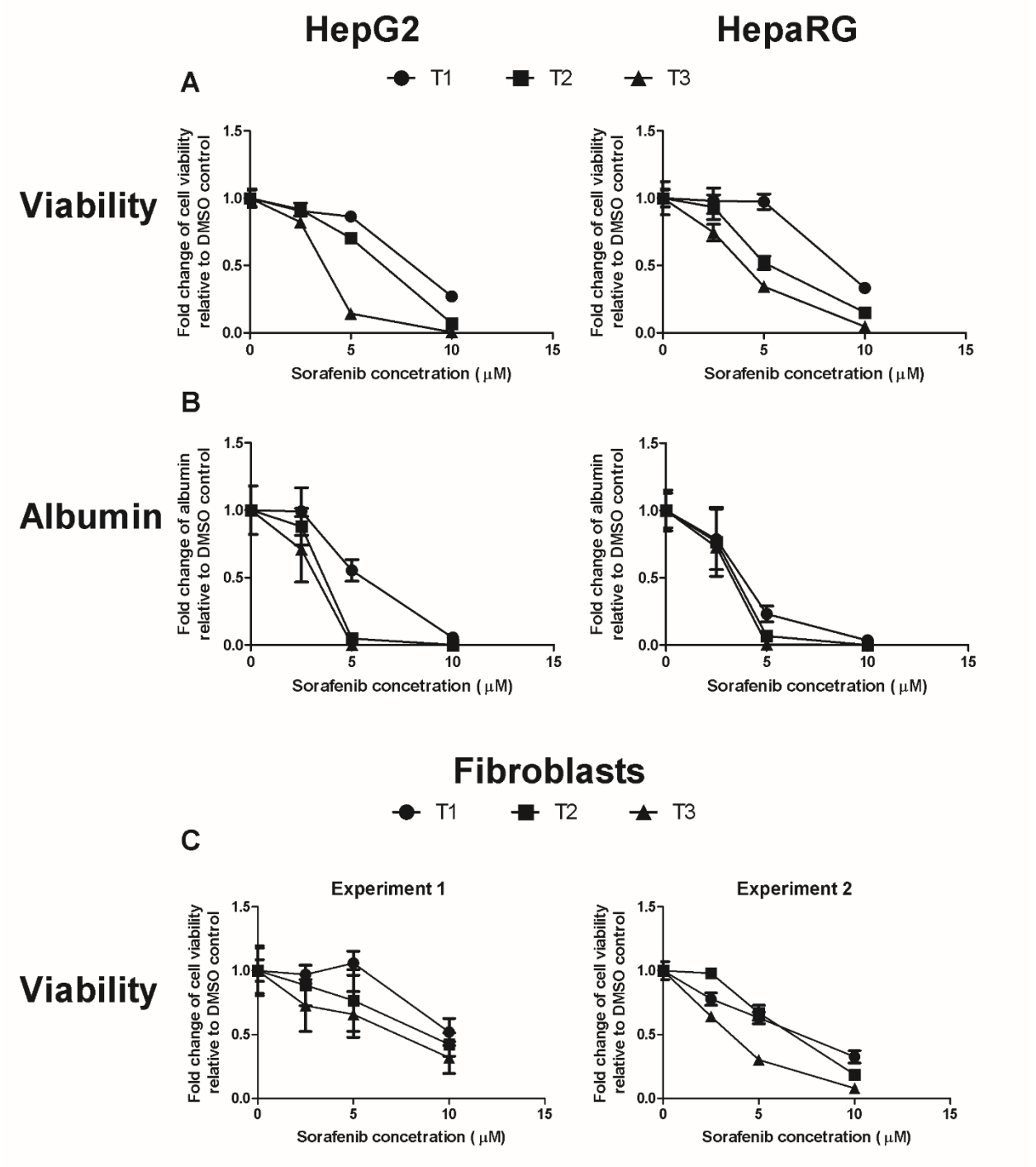

Figure 7. Treatment of MPCCs (containing either HepG2 or HepaRG liver cancer cell line) with sorafenib and assessment of MPCC viability (A) and albumin secretion (B) relative to DMSO-treated control cultures. Viability of fibroblast controls is in panel (C) across two experiments. T1, T2, and T3 are 2, 4, and 6 days after drug treatment, respectively.

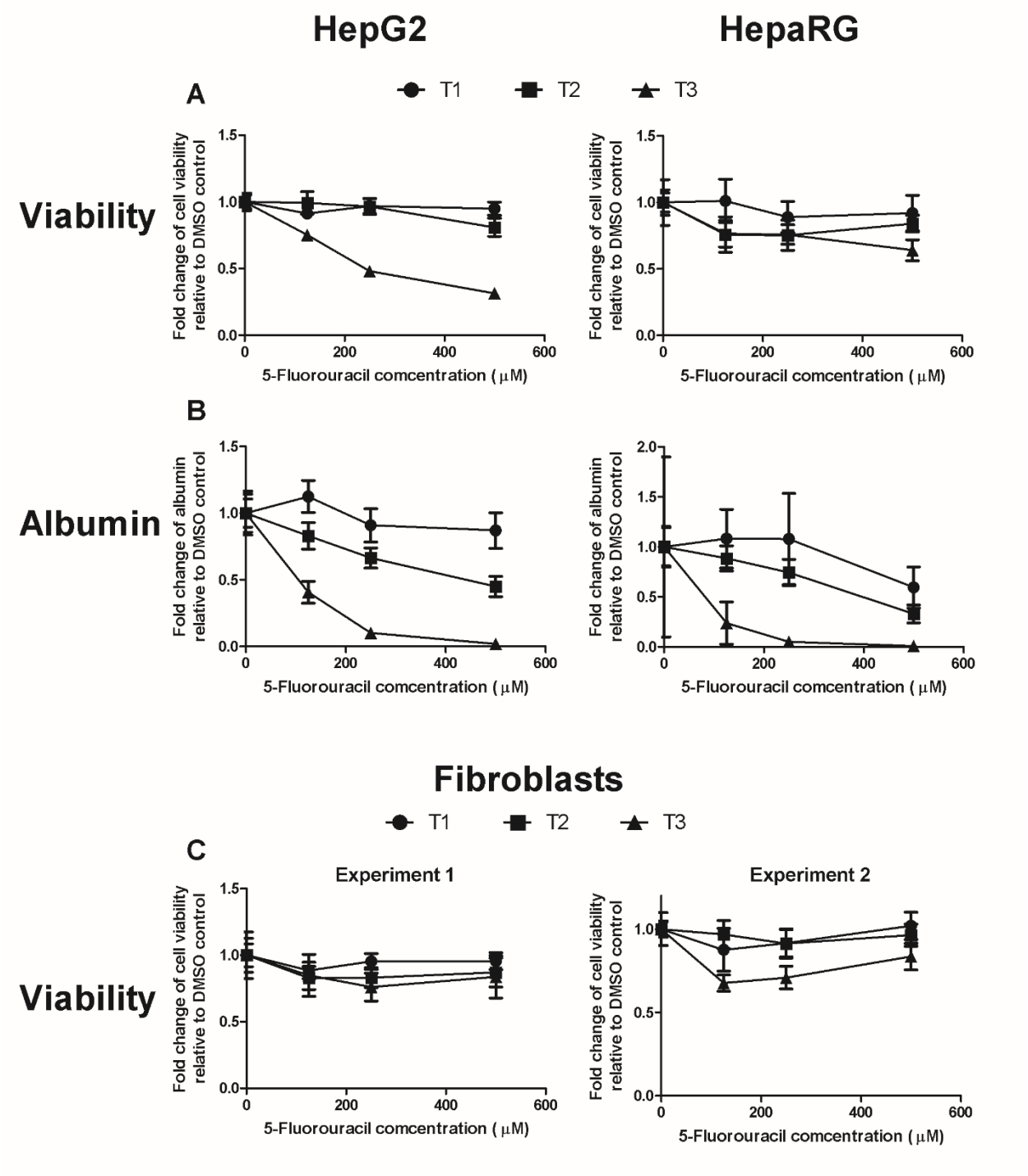

Figure 8. Treatment of MPCCs (containing either HepG2 or HepaRG liver cancer cell line) with 5-fluorouracil and assessment of MPCC viability (A) and albumin secretion (B) relative to DMSO-treated control cultures. Viability of fibroblast controls is in panel (C) across two experiments. T1, T2, and T3 are 2, 4, and 6 days after drug treatment, respectively.

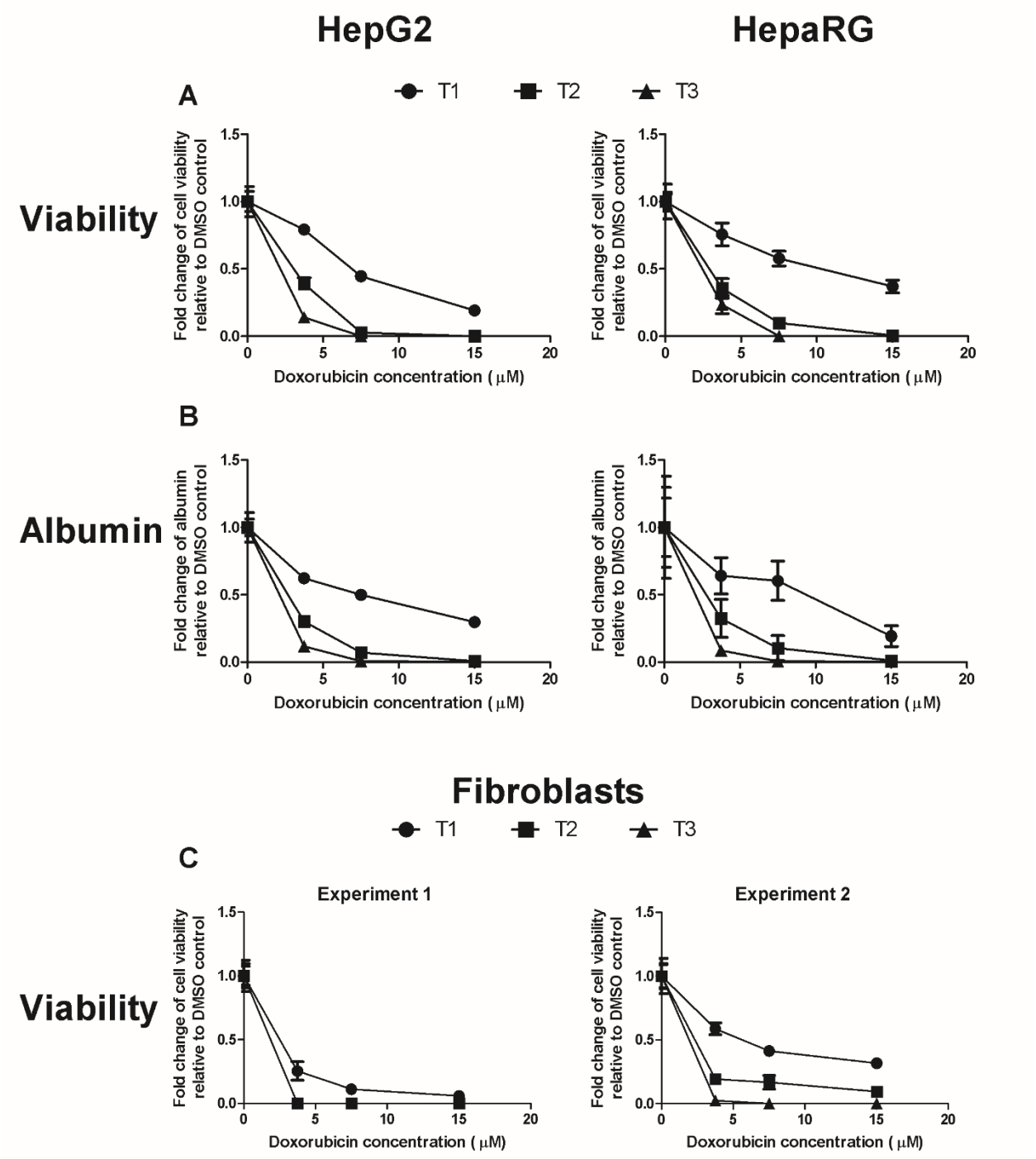

Figure 9. Treatment of MPCCs (containing either HepG2 or HepaRG liver cancer cell line) with doxorubicin and assessment of MPCC viability (A) and albumin secretion (B) relative to DMSO-treated control cultures. Viability of fibroblast controls is in panel (C) across two experiments. T1, T2, and T3 are 2, 4, and 6 days after drug treatment, respectively.

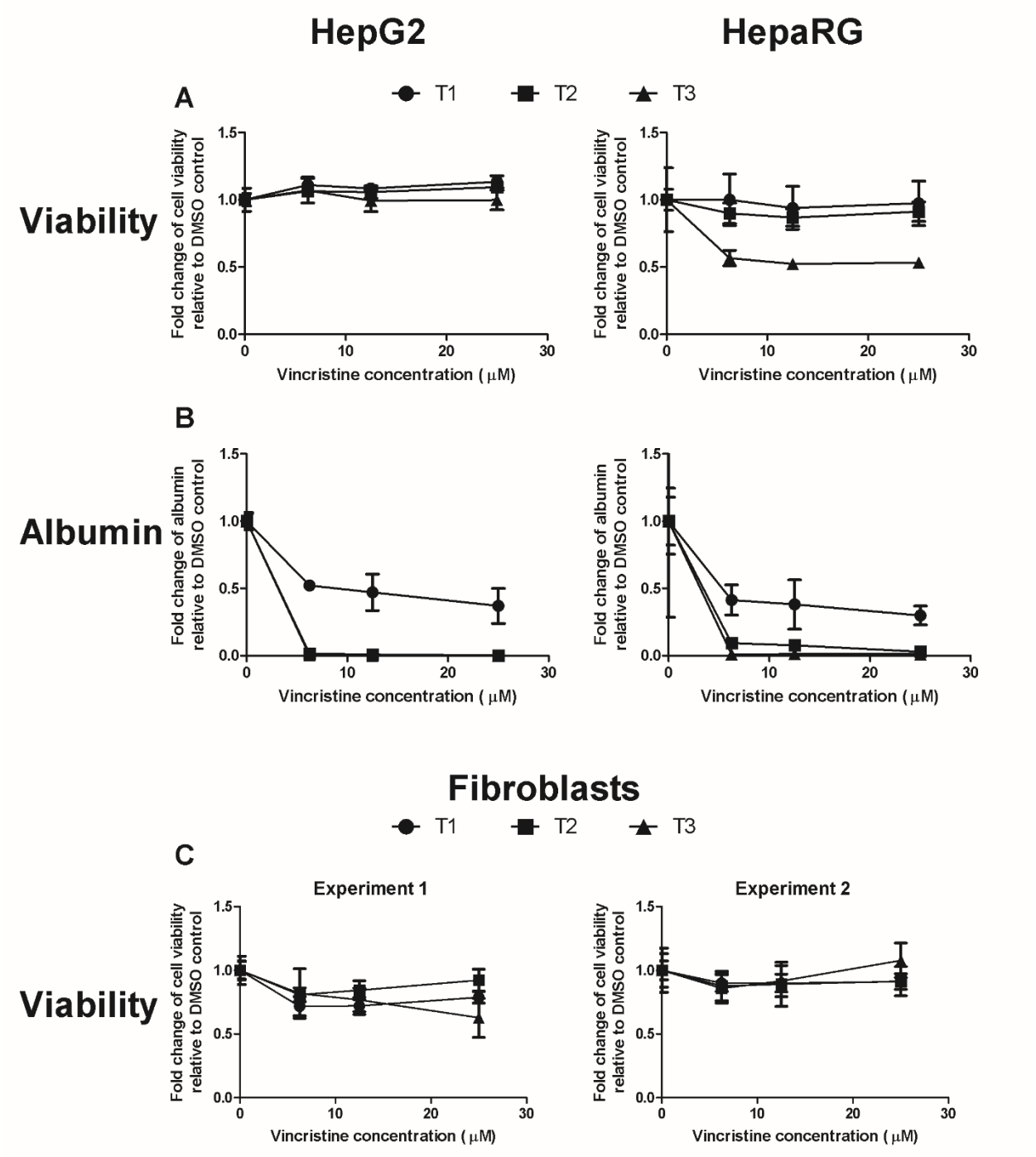

Figure 10. Treatment of MPCCs (containing either HepG2 or HepaRG liver cancer cell line) with vincristine and assessment of MPCC viability (A) and albumin secretion (B) relative to DMSO-treated control cultures. Viability of fibroblast controls is in panel (C) across two experiments. T1, T2, and T3 are 2, 4, and 6 days after drug treatment, respectively.

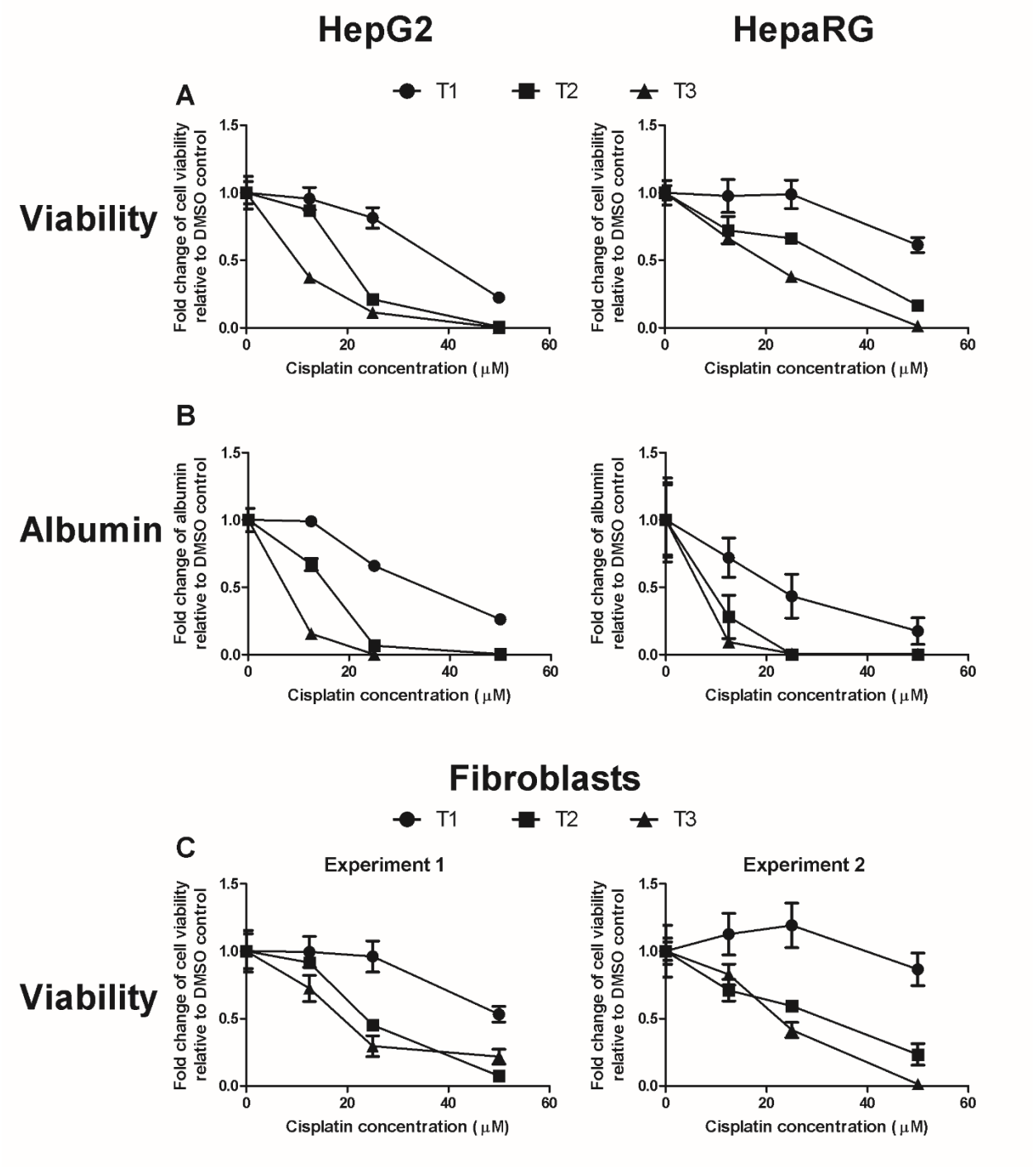

Figure 11. Treatment of MPCCs (containing either HepG2 or HepaRG liver cancer cell line) with cisplatin and assessment of MPCC viability (A) and albumin secretion (B) relative to DMSO-treated control cultures. Viability of fibroblast controls is in panel (C) across two experiments. T1, T2, and T3 are 2, 4, and 6 days after drug treatment, respectively.

1.5 REFERENCES

[1] A. Jemal, F. Bray, M.M. Center, J. Ferlay, E. Ward, D. Forman, Global cancer statistics, CA Cancer J Clin 61(2) (2011) 69-90.

[2] R.L. Siegel, K.D. Miller, A. Jemal, Cancer Statistics, 2017, CA Cancer J Clin 67(1) (2017) 7-30.

[3] S. Roessler, A. Budhu, X.W. Wang, Deciphering cancer heterogeneity: the biological space, Front Cell Dev Biol 2 (2014) 12.

[4] J.A. DiMasi, H.G. Grabowski, R.W. Hansen, Innovation in the pharmaceutical industry: New estimates of R&D costs, J Health Econ 47 (2016) 20-33.

[5] Improving and Accelerating Therapeutic Development for Nervous System Disorders: Workshop Summary, Washington (DC), 2014.

[6] M. Suggitt, M.C. Bibby, 50 years of preclinical anticancer drug screening: empirical to target-driven approaches, Clin Cancer Res 11(3) (2005) 971-81.

[7] L. Bakiri, E.F. Wagner, Mouse models for liver cancer, Mol Oncol 7(2) (2013) 206-23.

[8] D.A. Groneberg, C. Grosse-Siestrup, A. Fischer, In vitro models to study hepatotoxicity, Toxicol Pathol 30(3) (2002) 394-9.

[9] A. Sivaraman, J.K. Leach, S. Townsend, T. Iida, B.J. Hogan, D.B. Stolz, R. Fry, L.D. Samson, S.R. Tannenbaum, L.G. Griffith, A microscale in vitro physiological model of the liver: predictive screens for drug metabolism and enzyme induction, Curr Drug Metab 6(6) (2005) 569-91.

[10] J.J. Xu, P.V. Henstock, M.C. Dunn, A.R. Smith, J.R. Chabot, D. de Graaf, Cellular imaging predictions of clinical drug-induced liver injury, Toxicol Sci 105(1) (2008) 97-105.

[11] S.R. Khetani, S.N. Bhatia, Microscale culture of human liver cells for drug development, Nat Biotechnol 26(1) (2008) 120-6.

[12] S. March, V. Ramanan, K. Trehan, S. Ng, A. Galstian, N. Gural, M.A. Scull, A. Shlomai, M.M. Mota, H.E. Fleming, S.R. Khetani, C.M. Rice, S.N. Bhatia, Micropatterned coculture of primary human hepatocytes and supportive cells for the study of hepatotropic pathogens, Nat Protoc 10(12) (2015) 2027-53.

[13] M.D. Davidson, D.A. Kukla, S.R. Khetani, Microengineered cultures containing human hepatic stellate cells and hepatocytes for drug development, Integr Biol (Camb) 9(8) (2017) 662-677.

[14] B.R. Ware, M.J. Durham, C.P. Monckton, S.R. Khetani, A Cell Culture Platform to Maintain Long-term Phenotype of Primary Human Hepatocytes and Endothelial Cells, Cell Mol Gastroenterol Hepatol 5(3) (2018) 187-207.

[15] A. Takai, V. Fako, H. Dang, M. Forgues, Z. Yu, A. Budhu, X.W. Wang, Three-dimensional Organotypic Culture Models of Human Hepatocellular Carcinoma, Sci Rep 6 (2016) 21174.

[16] D. Yip, C.H. Cho, A multicellular 3D heterospheroid model of liver tumor and stromal cells in collagen gel for anti-cancer drug testing, Biochem Biophys Res Commun 433(3) (2013) 327-32.

[17] S.R. Khetani, C. Kanchagar, O. Ukairo, S. Krzyzewski, A. Moore, J. Shi, S. Aoyama, M. Aleo, Y. Will, Use of micropatterned cocultures to detect compounds that cause drug-induced liver injury in humans, Toxicol Sci 132(1) (2013) 107-17.

[18] F. van Zijl, G. Zulehner, M. Petz, D. Schneller, C. Kornauth, M. Hau, G. Machat, M. Grubinger, H. Huber, W. Mikulits, Epithelial-mesenchymal transition in hepatocellular carcinoma, Future Oncol 5(8) (2009) 1169-79.

[19] J. Seetharamappa, B.P. Kamat, Spectroscopic studies on the mode of interaction of an anticancer drug with bovine serum albumin, Chem Pharm Bull (Tokyo) 52(9) (2004) 1053-7.

[20] S. Bi, Y. Sun, C. Qiao, H. Zhang, C. Liu, Binding of several anti-tumor drugs to bovine serum albumin: Fluorescence study, Journal of Luminescence 129(5) (2009) 541-547.

[21] D.P. Aden, A. Fogel, S. Plotkin, I. Damjanov, B.B. Knowles, Controlled synthesis of HBsAg in a differentiated human liver carcinoma-derived cell line, Nature 282(5739) (1979) 615-6.

[22] B.B. Knowles, C.C. Howe, D.P. Aden, Human hepatocellular carcinoma cell lines secrete the major plasma proteins and hepatitis B surface antigen, Science 209(4455) (1980) 497-9.

[23] H. Hugo, M.L. Ackland, T. Blick, M.G. Lawrence, J.A. Clements, E.D. Williams, E.W. Thompson, Epithelial--mesenchymal and mesenchymal--epithelial transitions in carcinoma progression, J Cell Physiol 213(2) (2007) 374-83.

[24] C.L. Chaffer, E.W. Thompson, E.D. Williams, Mesenchymal to epithelial transition in development and disease, Cells Tissues Organs 185(1-3) (2007) 7-19.

[25] A. Wells, Y.L. Chao, J. Grahovac, Q. Wu, D.A. Lauffenburger, Epithelial and mesenchymal phenotypic switchings modulate cell motility in metastasis, Front Biosci (Landmark Ed) 16 (2011) 815-37.

[26] R. Kalluri, R.A. Weinberg, The basics of epithelial-mesenchymal transition, J Clin Invest 119(6) (2009) 1420-8.

[27] P. Gripon, S. Rumin, S. Urban, J. Le Seyec, D. Glaise, I. Cannie, C. Guyomard, J. Lucas, C. Trepo, C. Guguen-Guillouzo, Infection of a human hepatoma cell line by hepatitis B virus, Proc Natl Acad Sci U S A 99(24) (2002) 15655-60.

[28] R. Parent, M.J. Marion, L. Furio, C. Trepo, M.A. Petit, Origin and characterization of a human bipotent liver progenitor cell line, Gastroenterology 126(4) (2004) 1147-56.

[29] H. Nakabayashi, K. Taketa, K. Miyano, T. Yamane, J. Sato, Growth of human hepatoma cells lines with differentiated functions in chemically defined medium, Cancer Res 42(9) (1982) 3858-63.

[30] H. Nakamura, Y. Izumoto, H. Kambe, T. Kuroda, T. Mori, K. Kawamura, H. Yamamoto, T. Kishimoto, Molecular cloning of complementary DNA for a novel human hepatoma-derived growth factor. Its homology with high mobility group-1 protein, J Biol Chem 269(40) (1994) 25143-9.

[31] S. Wilkening, F. Stahl, A. Bader, Comparison of primary human hepatocytes and hepatoma cell line Hepg2 with regard to their biotransformation properties, Drug Metab Dispos 31(8) (2003) 1035-42.

[32] L. Adnane, P.A. Trail, I. Taylor, S.M. Wilhelm, Sorafenib (BAY 43-9006, Nexavar), a dual-action inhibitor that targets RAF/MEK/ERK pathway in tumor cells and tyrosine kinases VEGFR/PDGFR in tumor vasculature, Methods Enzymol 407 (2006) 597-612.

[33] S. Wilhelm, C. Carter, M. Lynch, T. Lowinger, J. Dumas, R.A. Smith, B. Schwartz, R. Simantov, S. Kelley, Discovery and development of sorafenib: a multikinase inhibitor for treating cancer, Nat Rev Drug Discov 5(10) (2006) 835-44.

[34] S.M. Wilhelm, C. Carter, L. Tang, D. Wilkie, A. McNabola, H. Rong, C. Chen, X. Zhang, P. Vincent, M. McHugh, Y. Cao, J. Shujath, S. Gawlak, D. Eveleigh, B. Rowley, L. Liu, L. Adnane, M. Lynch, D. Auclair, I. Taylor, R. Gedrich, A. Voznesensky, B. Riedl, L.E. Post, G. Bollag, P.A. Trail, BAY 43-9006 exhibits broad spectrum oral antitumor activity and targets the RAF/MEK/ERK pathway and receptor tyrosine kinases involved in tumor progression and angiogenesis, Cancer Res 64(19) (2004) 7099-109.

[35] M. Baccarini, Second nature: biological functions of the Raf-1 "kinase", FEBS Lett 579(15) (2005) 3271-7.

[36] A.J. Muslin, Role of raf proteins in cardiac hypertrophy and cardiomyocyte survival, Trends Cardiovasc Med 15(6) (2005) 225-9.

[37] G. Galabova-Kovacs, A. Kolbus, D. Matzen, K. Meissl, D. Piazzolla, C. Rubiolo, K. Steinitz, M. Baccarini, ERK and beyond: insights from B-Raf and Raf-1 conditional knockouts, Cell Cycle 5(14) (2006) 1514-8.

[38] J.H. Doroshow, Role of hydrogen peroxide and hydroxyl radical formation in the killing of Ehrlich tumor cells by anticancer quinones, Proc Natl Acad Sci U S A 83(12) (1986) 4514-8.

[39] K.M. Tewey, T.C. Rowe, L. Yang, B.D. Halligan, L.F. Liu, Adriamycin-induced DNA damage mediated by mammalian DNA topoisomerase II, Science 226(4673) (1984) 466-8.

[40] S. Dasari, P.B. Tchounwou, Cisplatin in cancer therapy: molecular mechanisms of action, Eur J Pharmacol 740 (2014) 364-78.

[41] D.B. Longley, D.P. Harkin, P.G. Johnston, 5-fluorouracil: mechanisms of action and clinical strategies, Nat Rev Cancer 3(5) (2003) 330-8.

[42] C.M. Walko, C. Lindley, Capecitabine: a review, Clin Ther 27(1) (2005) 23-44.

[43] S.B. Fox, A. Moghaddam, M. Westwood, H. Turley, R. Bicknell, K.C. Gatter, A.L. Harris, Platelet-derived endothelial cell growth factor/thymidine phosphorylase expression in normal tissues: an immunohistochemical study, J Pathol 176(2) (1995) 183-90.

[44] T. Tabata, M. Katoh, S. Tokudome, M. Hosakawa, K. Chiba, M. Nakajima, T. Yokoi, Bioactivation of capecitabine in human liver: involvement of the cytosolic enzyme on 5'-deoxy-5-fluorocytidine formation, Drug Metab Dispos 32(7) (2004) 762-7.

[45] C.E. Gidding, S.J. Kellie, W.A. Kamps, S.S. de Graaf, Vincristine revisited, Crit Rev Oncol Hematol 29(3) (1999) 267-87.

[46] N.S. el Saghir, K.A. Hawkins, Hepatotoxicity following vincristine therapy, Cancer 54(9) (1984) 2006-8.

[47] A.V. Roschke, G. Tonon, K.S. Gehlhaus, N. McTyre, K.J. Bussey, S. Lababidi, D.A. Scudiero, J.N. Weinstein, I.R. Kirsch, Karyotypic complexity of the NCI-60 drug-screening panel, Cancer Res 63(24) (2003) 8634-47.

[48] V.C. Daniel, L. Marchionni, J.S. Hierman, J.T. Rhodes, W.L. Devereux, C.M. Rudin, R. Yung, G. Parmigiani, M. Dorsch, C.D. Peacock, D.N. Watkins, A primary xenograft model of small-cell lung cancer reveals irreversible changes in gene expression imposed by culture in vitro, Cancer Res 69(8) (2009) 3364-73.

[49] K.M. Tveit, A. Pihl, Do cell lines in vitro reflect the properties of the tumours of origin? A study of lines derived from human melanoma xenografts, Br J Cancer 44(6) (1981) 775-86.

[50] T.T. Chang, M. Hughes-Fulford, Monolayer and spheroid culture of human liver hepatocellular carcinoma cell line cells demonstrate distinct global gene expression patterns and functional phenotypes, Tissue Eng Part A 15(3) (2009) 559-67.

[51] H.R. Jung, H.M. Kang, J.W. Ryu, D.S. Kim, K.H. Noh, E.S. Kim, H.J. Lee, K.S. Chung, H.S. Cho, N.S. Kim, D.S. Im, J.H. Lim, C.R. Jung, Cell Spheroids with Enhanced Aggressiveness to Mimic Human Liver Cancer In Vitro and In Vivo, Sci Rep 7(1) (2017) 10499.

[52] Y. Miyauchi, K. Yasuchika, K. Fukumitsu, T. Ishii, S. Ogiso, T. Minami, H. Kojima, R. Yamaoka, H. Katayama, T. Kawai, E.Y. Yoshitoshi-Uebayashi, S. Kita, K. Yasuda, N. Sasaki, S.

Uemoto, A novel three-dimensional culture system maintaining the physiological extracellular matrix of fibrotic model livers accelerates progression of hepatocellular carcinoma cells, Sci Rep 7(1) (2017) 9827.

[53] A. Skardal, M. Devarasetty, C. Rodman, A. Atala, S. Soker, Liver-Tumor Hybrid Organoids for Modeling Tumor Growth and Drug Response In Vitro, Ann Biomed Eng 43(10) (2015) 2361-73.

[54] X.X. Xu, C. Liu, Y. Liu, N. Li, X. Guo, S.J. Wang, G.W. Sun, W. Wang, X.J. Ma, Encapsulated human hepatocellular carcinoma cells by alginate gel beads as an in vitro metastasis model, Exp Cell Res 319(14) (2013) 2135-44.

[55] F. Heindryckx, P. Gerwins, Targeting the tumor stroma in hepatocellular carcinoma, World J Hepatol 7(2) (2015) 165-76.

[56] T. Amann, F. Bataille, T. Spruss, M. Muhlbauer, E. Gabele, J. Scholmerich, P. Kiefer, A.K. Bosserhoff, C. Hellerbrand, Activated hepatic stellate cells promote tumorigenicity of hepatocellular carcinoma, Cancer Sci 100(4) (2009) 646-53.

[57] C. Coulouarn, A. Corlu, D. Glaise, I. Guenon, S.S. Thorgeirsson, B. Clement, Hepatocyte-stellate cell cross-talk in the liver engenders a permissive inflammatory microenvironment that drives progression in hepatocellular carcinoma, Cancer Res 72(10) (2012) 2533-42.

[58] S. Coulon, F. Heindryckx, A. Geerts, C. Van Steenkiste, I. Colle, H. Van Vlierberghe, Angiogenesis in chronic liver disease and its complications, Liver Int 31(2) (2011) 146-62.

[59] D. Capece, M. Fischietti, D. Verzella, A. Gaggiano, G. Cicciarelli, A. Tessitore, F. Zazzeroni, E. Alesse, The inflammatory microenvironment in hepatocellular carcinoma: a pivotal role for tumor-associated macrophages, Biomed Res Int 2013 (2013) 187204.

[60] S.R. Khetani, D.R. Berger, K.R. Ballinger, M.D. Davidson, C. Lin, B.R. Ware, Microengineered liver tissues for drug testing, J Lab Autom 20(3) (2015) 216-50.

CHAPTER 2. HUMAN CHOLANGIOCYTE MODEL

2.1 INTRODUCTION

2.1.1 Importance of hepatocyte and cholangiocyte in liver

Liver is a highly metabolic organ comprised of two epithelial cell types. The main epithelial cell type in the liver is called the hepatocyte, which account for about 70% of total cells in liver (**Figure 1**). Hepatocyte contributes to protein synthesis, metabolism, and detoxification in the human body and it has been used for research of liver physiology, pathology, and chronic drug screening. However, the problem with conventional hepatocyte cultures *in vitro* is that hepatocyte lose function rapidly in 2D monolayers [1]. There is a need to create a culture platform to stabilize and support hepatocyte *in vitro*. The other cell type of the liver epithelial cell is cholangiocyte, which lines the bile duct system (**Figure 1**). Although cholangiocytes only comprise about 3% to 5% of the total cells in liver, they play an important role of liver physiology, regeneration, and pathology [2, 3]. The main function of cholangiocytes is bile secretion and transport, which are regulated by many transporters such as water channels and $Cl^-/HCO3^-$ exchangers [4]. Another function of cholangiocytes may be related to the interaction with other cell types such as hepatocytes. Generally, cholangiocytes in the liver are maintained in a quiescent (non-proliferative) state [3]. However, liver injury can cause bile duct injury, impair hepatocyte proliferation, and cause cholangiocytes to become activated and proliferate. Cholangiocyte proliferation, also called ductular reaction, is thought to be associated with several liver diseases such as liver fibrosis [5]. Therefore, hepatocytes and cholangiocytes are both very crucial in liver research and it is important to model their heterotypic interactions

in vitro. Moreover, since cholangiocytes are the targets of many liver diseases, the model may be used to develop a liver disease model for drug screening purposes.

2.1.2 Research on hepatocytes and cholangiocytes

As described above, hepatocytes cannot be stabilized in 2D conventional cultures. To improve hepatocyte culture and maintain their functions over at least a few weeks in culture, the micropatterned co-culture (MPCC) platform was used to co-culture primary human hepatocytes (PHHs) with 3T3-J2 murine embryonic fibroblasts, which can support and stabilize hepatocytes [6]. This culture platform has been shown to maintain hepatic functions for 4-6 weeks. However, it is not clear if cholangiocytes can be incorporated into the MPCC model towards modeling hepatocyte-cholangiocyte interactions. Another method co-cultured PHHs with rat liver epithelial cells, which enhanced hepatocyte functions [7]. However, rat liver epithelial cells are considered to be unrelated to bile duct cells. Besides, rat cells and human cells maintain key species-species differences in metabolic pathways [8, 9]. In another study, Schlosser et al. showed that increased [$Ca2^{+}$] in hepatocytes could increase [$Ca2^{+}$] in bile duct cells and other hepatocytes [10]. Finally, Liu et al. showed that hepatocytes could be derived from cholangiocytes when hepatocyte proliferation was inhibited [11]. They created an *in vivo* mouse model that caused liver injury and inhibited hepatocyte proliferation; in this model, cholangiocytes transdifferentiated into hepatocytes. Despite the above-discussed progress in modeling interactions of hepatocytes and cholangiocytes, there remains a need for a human-relevant model that can be used to mimic *in vivo*-like interactions between PHHs and primary human cholangiocytes towards modeling disease phenotypes for drug discovery/screening.

2.1.3 Purpose of the study

In this study, we sought to create a culture platform that can be used to support and maintain PHH and cholangiocyte viability and functions as well as to understand the interaction of these two cell types. Specifically, we utilized the MPCC platform to create co-cultures of hepatocytes and cholangiocytes (C-MPCCs) to determine if cholangiocytes could support/stabilize hepatic functions *in vitro*. In addition, since 3T3-J2 fibroblasts have been previously shown to support hepatocyte functions for several weeks, we created hepatocyte/cholangiocyte/fibroblast tri-cultures (C-MPTCs) to compare and contrast with the C-MPCC model. Morphology and functional markers were measured in the culture platforms to determine the effects on cell phenotypes.

2.2 MATERIALS AND MATHODS

2.2.1 Cholangiocyte culture

Cryopreserved cholangiocyte vials were purchased from ZenBio (Research Triangle Park, NC). Cells were cultured and passaged with cholangiocyte culture medium comprised of Dulbecco's Modified Eagle's Medium/ F-12 50/50 (DMEM/ F-12, Corning), 10% of bovine serum (Life Technologies, Carlsbad, CA), 1% vol/vol penicillin-streptomycin (Corning Cellgro), hydrocortisone (2.5µg/mL), insulin (5µg/mL), and epidermal growth factor (EGF, 10ng/mL). Cholangiocytes were thawed in 37°C water bath for 120 seconds and diluted in10 mL cholangiocyte culture medium. Then, the cell suspension of cholangiocytes was spun at 200xg for 5 minutes. The supernatant was discarded and the cells were re-suspended in cholangiocyte culture medium. Cholangiocytes were then cultured in flasks with manufacturer recommended cell density, and culture medium was changed every other day.

2.2.2 Micropatterened co-cultures and tri-cultures

Cryopreserved PHHs were commercially obtained from Triangle Research Labs (Durham, NC). PHHs were thawed, counted, and viability was assessed as previously described [12]. MPCCs were created as described in chapter 1. Briefly, PHHs were seeded onto collagen patterned wells of 24-well plates. After PHHs had spread to fill in the collagen domains, the cultures were incubated with collagen to coat the remaining surface area to enable attachment of cholangiocytes. The next day, cell suspension of fibroblasts (for MPCCs), cholangiocytes (for C-MPCCs) or fibroblasts mixed with cholangiocytes (for C-MPTCs) were seeded at ~60k cells per well of a 24-wells plate onto the micropatterned PHH colonies. The ratios of fibroblasts and

cholangiocytes in C-MPTCs were 50:50 fibroblasts/cholangiocytes, 75:25 fibroblasts/cholangiocytes and 97:3 fibroblasts/cholangiocytes (approximate ratio in the liver [13]).

2.2.3 Quantification of cell functions

Culture supernatants were collected and assessed for albumin and urea concentrations using previously described methods [6]. Briefly, albumin was measured as described in chapter 1 and urea production was measured by a colorimetric reaction with diacetyl monoxime, acid, and heat (kit from Stanbio Labs, Boerne, TX). Cytochrome P-450 (CYP450) enzyme activities were measured by first incubating the cultures with substrate for 1 or 3 hours at 37°C and then detecting either the luminescence or fluorescence of metabolites. CYP2A6 enzyme activity was measured as described in chapter 1. CYP1A2 enzyme activity was measured by metabolism of 7-ethoxyresorufin to fluorescent resorufin (Sigma-Aldrich, St. Louis, MO). CYP2C9 enzyme activity was measured by cleavage of luciferin-H into luminescent luciferin (Promega, Madison, WI). CYP3A4 enzyme activity was measured by cleavage of luciferin-IPA into luminescent luciferin (Promega).

2.2.4 Data analysis

Each experiment was carried out in triplicate wells for each condition. Microsoft Excel and GraphPad Prism (La Jolla, CA) were used for analyzing and graphing data. Error bars on graphs represent standard deviations for each condition. Statistical significance was determined using two-way analysis of variance (ANOVA) with a Bonferroni test.

2.3 RESULTS

2.3.1 Morphology of hepatocyte/cholangiocyte co-cultures relative to hepatocyte/fibroblast co-cultures and hepatocyte mono-cultures

Cholangiocytes could be co-cultured with PHHs (C-MPCCs) and C-MPCCs were compared with patterned PHH mono-cultures (MPHs) and MPCCs containing PHHs and 3T3-J2 fibroblasts (**Figure 2**). Hepatocytes in both MPCCs (**Figure 3A and 3D**) and C-MPCCs (**Figure 3B and 3E**) could maintain prototypical hepatic morphology and pattern fidelity for at least three weeks. In addition, both co-cultures formats displayed lipid accumulation. In contrast, PHHs lost prototypical morphology and the patterns dissipated over two weeks (**Figure 3C and 3F**).

2.3.2 Functions of hepatocyte/cholangiocyte co-cultures relative to hepatocyte/fibroblast co-cultures and hepatocyte mono-cultures

At the functional level (**Figure 4**), MPCCs had stable and higher functions over three weeks as compared to C-MPCCs and MPHs. Cholangiocytes could not support PHHs in C-MPCCs to the same extent as the fibroblasts (as in MPCCs) at the functional level; however, the C-MPCCs were able to maintain higher hepatic functions over the MPHs throughout the culture period. For albumin secretions (**Figure 4A**), C-MPCCs had statistically similar levels as MPCCs and higher levels than MPHs for ~19 days. For urea secretions (**Figure 4B**), both C-MPCCs and MPHs had lower levels than MPCCs; however, the urea levels in C-MPCCs increased after two weeks as compared to MPHs, though did not reach the same levels as those measured in MPCCs. For CYP1A2 enzyme, MPCCs and C-MPCCs had similar activities (**Figure 4C**) and both models had higher activities than MPHs. In contrast, MPCCs had higher CYP2A6 activity

(**Figure 4D**), CYP2C9 activity (**Figure 4E**), and CYP3A4 activity (**Figure 4F**) than C-MPCCs and MPHs. Nonetheless, CYP2C9 activity in C-MPCCs (**Figure 4E**) increased after two weeks and CYP3A4 activity (**Figure 4F**) increased after three weeks. The above-discussed results/trends suggest that cholangiocytes can support PHH functions to a certain extent, but not to the same extent as the 3T3-J2 fibroblasts.

2.3.3 Morphology of hepatocyte/cholangiocyte/fibroblast tri-cultures relative to hepatocyte/fibroblast co-cultures

As discussed above, since cholangiocytes could not optimally support PHH functions, we created a tri-culture model in which micropatterned PHH colonies were co-cultured with a mixture of cholangiocytes and fibroblasts at different ratios (C-MPTCs, **Figure 5**). The morphology of PHHs and pattern fidelity could be maintained for at least three weeks in C-MPTCs (**Figure 6**). However, relative to MPCCs (**Figure 3A and 3D**), C-MPTCs displayed more microvascular steatosis (lipid accumulation) after three weeks, which is reminiscent of a non-alcoholic steatohepatitis (NASH) phenotype [14].

2.3.4 Functions of hepatocyte/cholangiocyte/fibroblast tri-cultures relative to hepatocyte/fibroblast co-cultures

For albumin secretions (**Figure 7A**), the highest ratio of fibroblasts to cholangiocytes in C-MPTCs (3:97 cholangiocyte:fibroblast) showed higher levels than MPCCs without cholangiocytes. For urea secretion, the highest ratio of fibroblasts to cholangiocytes did not lead to levels to the same magnitude as MPCCs (**Figure 7B**). For CYP450 enzyme activities, except for CYP1A2 (**Figure 7C**), increasing numbers of cholangiocytes in C-MPTCs led to

downregulation of CYP2A6 (**Figure 7D**), CYP2C9 (**Figure 7E**), and CYP3A4 activities (**Figure 7F**). Furthermore, CYP450 activities in C-MPTCs were lower (statistically) than MPCCs.

2.4 DISCUSSION

In this study, we developed two culture platforms, one in which micropatterned PHHs were co-cultured with cholangiocytes only (C-MPCCs), while another in which micropatterned PHHs were co-cultured with a mixture of cholangiocytes and 3T3-J2 fibroblasts at different ratios in a tri-culture configuration (C-MPTCs). We found that PHHs maintained morphology in C-MPCCs and hepatic functions were enhanced relative to MPHs; however, functions were significantly lower in C-MPCCs than in MPCCs containing only 3T3-J2 fibroblasts, which suggest that cholangiocytes can induce functions in PHHs relative to MPHs but not to the same extent as 3T3-J2 fibroblasts. Furthermore, C-MPTCs containing all three cell types displayed lower functions than MPCCs, with CYP1A2 activity being the exception, and functions in C-MPTCs were down-regulated with increasing numbers of cholangiocytes relative to the number of fibroblasts. Moreover, more microvascular steatosis in hepatocytes was observed in C-MPTCs as compared to MPCCs and C-MPCCs, which suggests that the C-MPTC model could potentially be useful as a model of liver disease (e.g. NASH).

Clement et al. previously showed induction of PHH functions in co-culture with rat liver epithelial cells [7]. However, it is not clear if rat liver epithelial cells used in that study were cholangiocytes. Thus, our study constitutes the first time that cholangiocytes have been shown to induce any functions in PHHs *in vitro* relative to rapidly declining PHH mono-cultures. The inhibition of hepatic functions (e.g. CYP3A4 activity) in C-MPTCs with increasing numbers of cholangiocytes relative to MPCC controls could be partially due to the reduced numbers of fibroblasts for supporting PHHs optimally. However, such inhibition could also be due to the effects of activated cholangiocytes on PHH functions as previously observed in

hepatocyte/human stellate cell/fibroblast tri-cultures [14]. Human stellate cells are thought to cause liver fibrosis upon activation into myofibroblasts that secrete extracellular matrix proteins (e.g. collagen I) following injury to the liver (e.g. NASH) [15, 16]. While the exact mechanisms underlying inhibition of hepatic functions in C-MPTCs is not entirely clear, to our knowledge, we are the first group to show such an effect *in vitro*. Furthermore, it has been reported that human cholangiocytes may need fibroblasts to maintain their viability [17]. In our study, higher number of fibroblasts may support the cholangiocyte phenotype, though further assessments of cholangiocyte phenotypic markers would be needed to test this hypothesis. We also found that co-culture with PHHs reciprocally changed cholangiocyte morphology since in pure monolayers, cholangiocytes were larger in size and spread out, whereas in co-cultures, they tended to be more elongated and packed in.

Normal cholangiocytes in the liver are typically quiescent (non-proliferative) [3, 18, 19]. These quiescent cholangiocytes are difficult to culture *in vitro* [20, 21] and our own studies showed a low cholangiocyte growth rate in pure monolayers (data not show). However, cholangiocyte proliferation, also called ductular reaction, can be induced by several factors including bile acids, hormones, growth factors and some signaling pathways such as cAMP-related pathways and Ca2+ related pathways *in vitro* or *in vivo* [5, 17, 22-24]. Under normal conditions, cholangiocyte proliferation is triggered to repair injured cells and support impaired functions. At the same time, cholangiocyte apoptosis is also increased. When cholangiocyte proliferation and apoptosis cannot maintain an equilibrium, it can cause liver disease [25-27]. Additionally, livers of patients with NASH [28], alcoholic liver disease [29] and hepatitis C viral infection [30] have all been shown to exhibit increased cholangiocyte proliferation. In this study,

we qualitatively observed cholangiocyte growth over time in C-MPTCs. Furthermore, we also observed microvascular steatosis in PHHs within C-MPTCs relative to C-MPCCs and MPCCs. Similar results were described in a previous study that utilized hepatocyte/human stellate cell/fibroblast tri-cultures, which mimicked a NASH phenotype [14]. Therefore, the hepatic dysfunctions, including steatosis and reduced CYP450 activities, and cholangiocyte proliferation in C-MPTCs may constitute a liver disease phenotype that can be potentially exploited for drug discovery in the future. However, further molecular profiling of the cultures would be required to determine the exact nature of the diseased phenotype relative to clinical liver samples.

The 2D C-MPTC platform provides a straight-forward strategy to observe the morphology of three cell types using standard light microscopy, all the while inducing hepatic functions relative to MPH controls. However, our 2D platform is not able to recapitulate the ductular structures formed by cholangiocytes *in vivo*. Duct-like structures have been observed in 3D cultures utilizing human-induced pluripotent stem cell-derived cholangiocytes [31] and normal human cholangiocytes [32]. We plan to build a 3D C-MPTC model in future studies to determine effects on cholangiocyte reorganization into duct-like structures. Additionally, since mouse fibroblasts do not entirely mimic human biology, we plan to pursue C-MPTCs created using portal human liver fibroblasts, which are found in the liver surrounding bile ducts and can regulate cholangiocyte proliferation via deposition of hyaluronic acid and other extracellular matrix proteins [33-35]. Such a revised model containing portal fibroblasts could also be used to understand their role in causing liver fibrosis by activation into myofibroblasts following liver injury [36-38]. Indeed, fibrosis, which often results from many liver diseases, typically develops from the portal area of the liver where cholangiocytes and portal fibroblasts reside [39-41].

In conclusion, we showed in this study that cholangiocytes can support some hepatic functions but not to the same extent as 3T3-J2 fibroblasts. Furthermore, tri-cultures containing PHHs, fibroblasts, and cholangiocytes led to hepatic dysfunctions (e.g. steatosis and CYP450 activity inhibition) as well as cholangiocyte proliferation that were reminiscent of a liver fibrosis/NASH phenotype. We anticipate that such a culture platform can be potentially useful as a drug screening tool in the future and to understand PHH-cholangiocyte interactions in liver pathology.

FIGURES

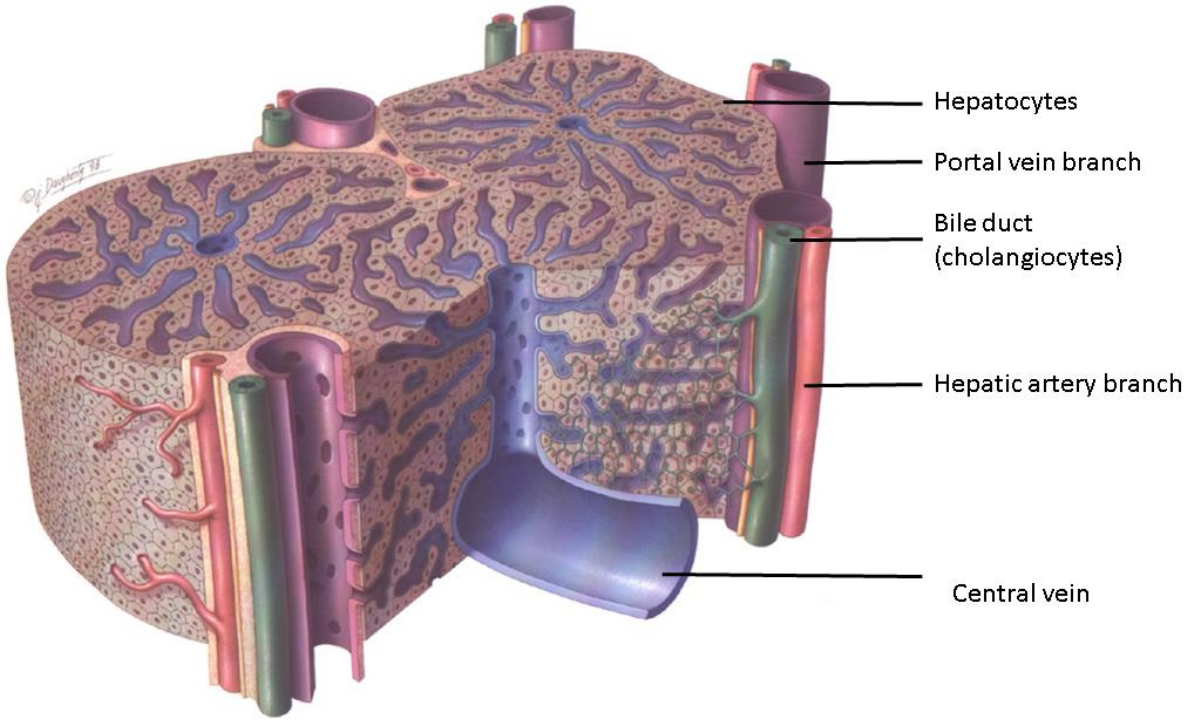

Figure 1. Architecture of two adjacent liver lobules, the repeating units in the liver. From [42].

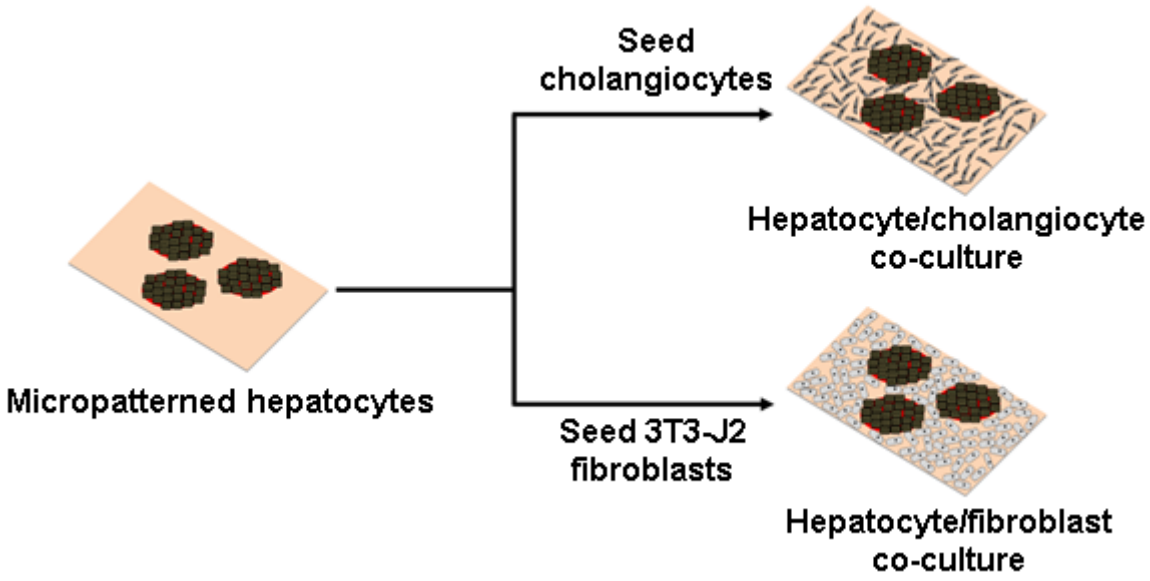

Figure 2. Schematic of co-cultures models from [43]. PHHs attached to collagen islands and were co-cultured with fibroblasts or cholangiocytes in the surrounding areas.

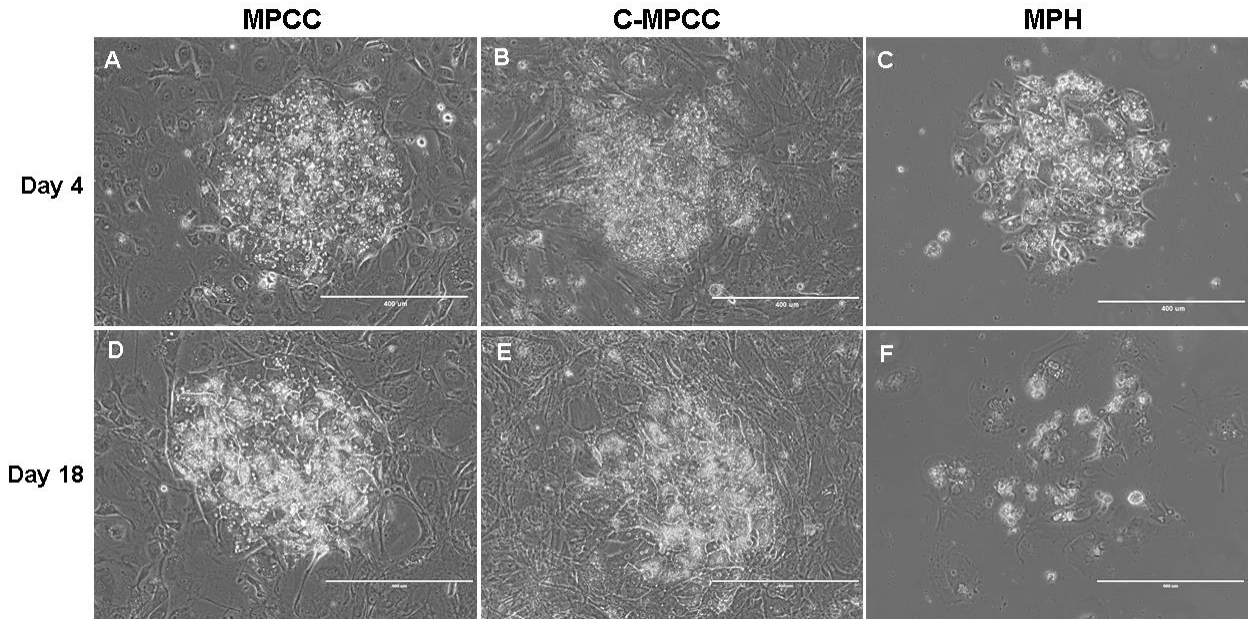

Figure 3. Morphology of MPCCs and C-MPCCs relative to MPHs. MPCC (left) and C-MPCC (middle) maintained morphology of PHHs over 18 days of culture as compared to declining morphology in MPHs (right). Lipid accumulation (white area) was observed in both MPCCs and C-MPCCs. All scale bars = 400 µm.

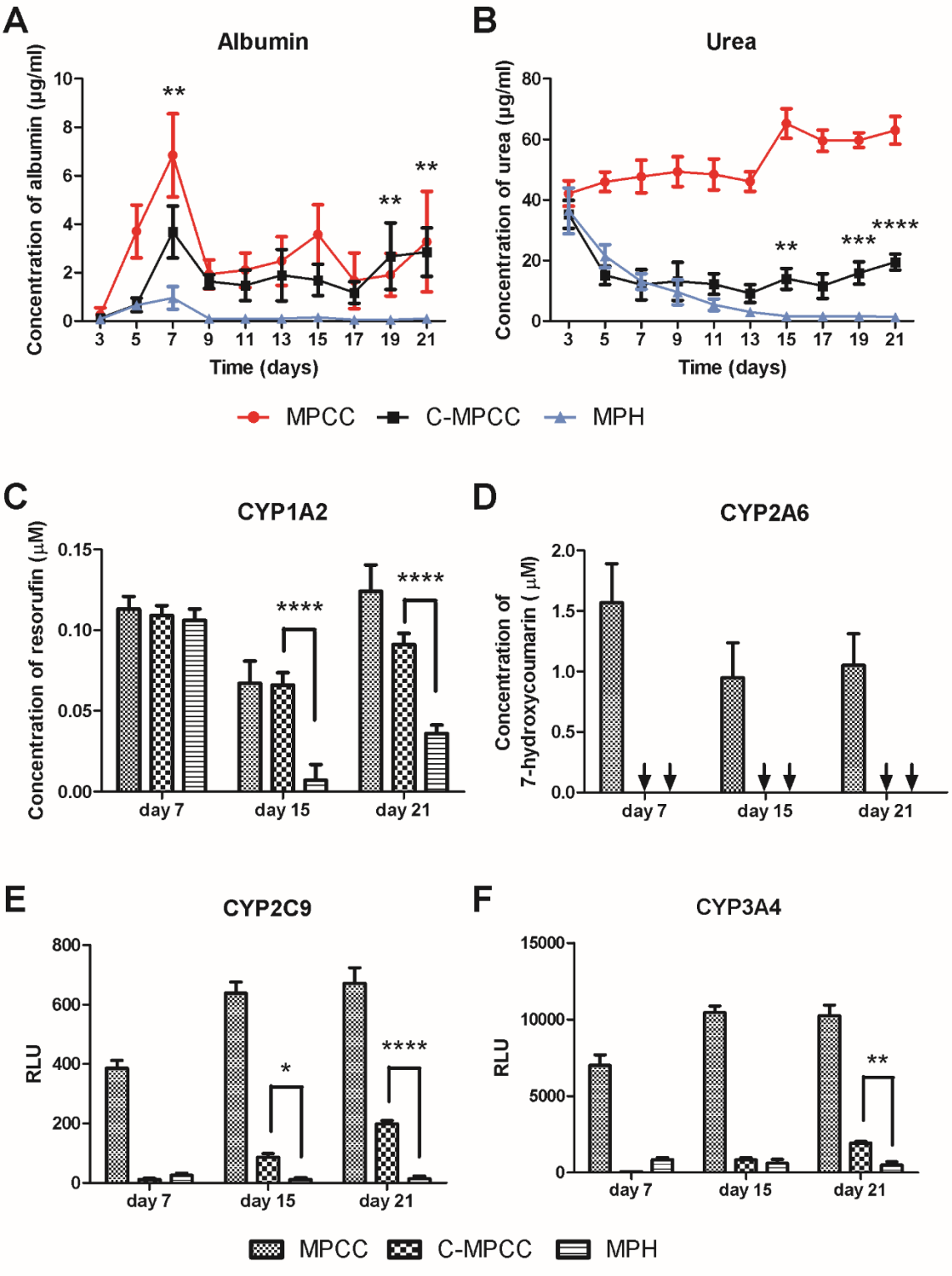
A
Albumin
Concentration of albumin (µg/ml)
Time (days)
B
Urea
Concentration of urea (µg/ml)
Time (days)
MPCC
C-MPCC
MPH
C
CYP1A2
Concentration of resorufin (µM)
day 7
day 15
day 21
D
CYP2A6
Concentration of 7-hydroxycoumarin (µM)
day 7
day 15
day 21
E
CYP2C9
RLU
day 7
day 15
day 21
F
CYP3A4
RLU
day 7
day 15
day 21
MPCC
C-MPCC
MPH

Figure 4. Functions of co-culture models relative to MPHs including (A) albumin secretion, (B) urea production, (C) CYP1A2 enzyme activity, (D) CYP2A6 activity, (E) CYP2C9 activity, and (F) CYP3A4 activity. Statistic significant showed the comparison of C-MPCCs and MPHs. Arrows indicate undetectable data. $*P < 0.05$, $**P < 0.01$, $***P < 0.001$ and $****P < 0.0001$.

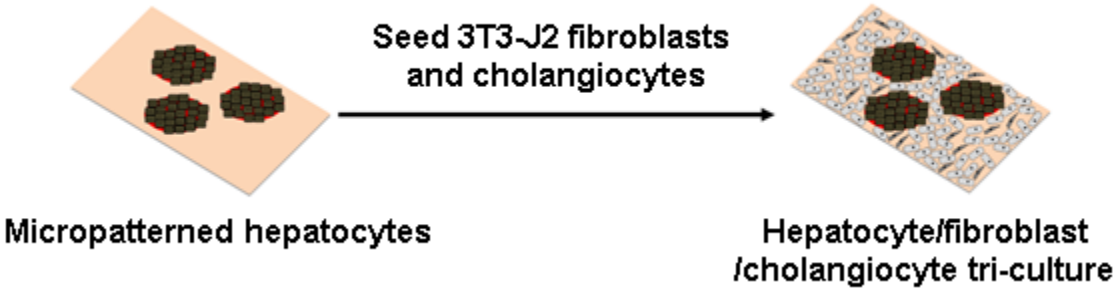

Figure 5. Schematic of tri-culture models from [44]. PHHs attached to collagen islands and were co-cultured with a mixture of fibroblasts and cholangiocytes at different ratios in the surrounding areas. Ratios tested were 50:50, 25:75, and 3:97 cholangiocytes:fibroblasts.

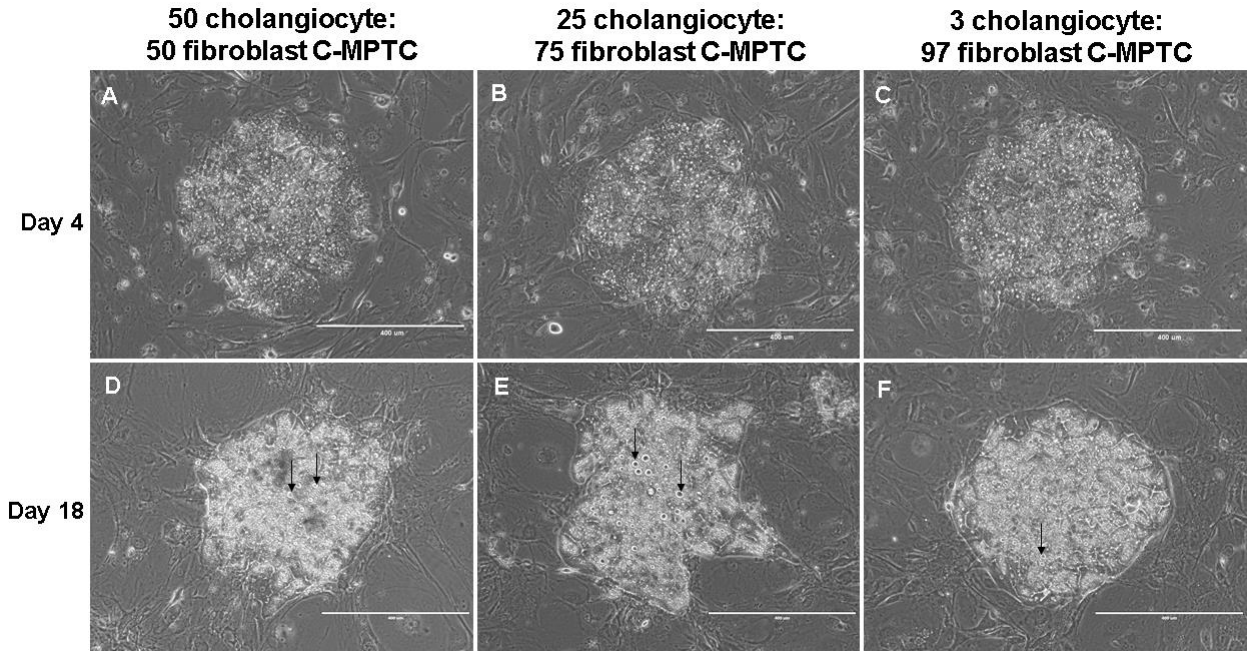

Figure 6. Morphology of C-MPTCs over 18 days. Arrows point to the microvascular steatosis. All scale bars = 400 µm.

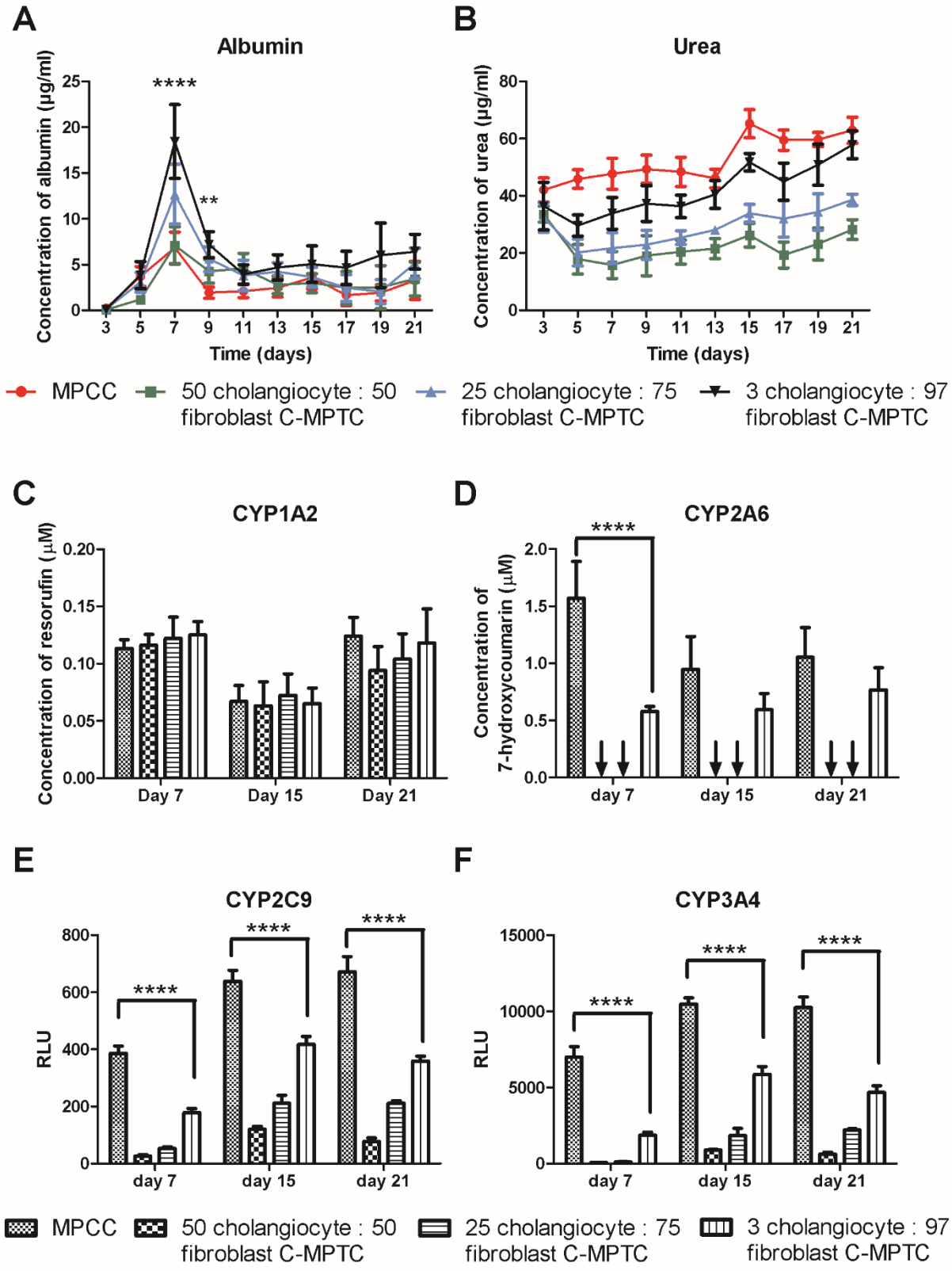
A
Albumin
Concentration of albumin (µg/ml)
Time (days)
****
**
B
Urea
Concentration of urea (µg/ml)
Time (days)
MPCC
50 cholangiocyte : 50 fibroblast C-MPTC
25 cholangiocyte : 75 fibroblast C-MPTC
3 cholangiocyte : 97 fibroblast C-MPTC
C
CYP1A2
Concentration of resorufin (µM)
Day 7
Day 15
Day 21
D
CYP2A6
Concentration of 7-hydroxycoumarin (µM)
****
day 7
day 15
day 21
E
CYP2C9
RLU
****
****
****
day 7
day 15
day 21
F
CYP3A4
RLU
****
****
****
day 7
day 15
day 21
MPCC
50 cholangiocyte : 50 fibroblast C-MPTC
25 cholangiocyte : 75 fibroblast C-MPTC
3 cholangiocyte : 97 fibroblast C-MPTC

Figure 7. Functions of tri-culture models relative to MPCCs including (A) albumin secretion, (B) urea production, (C) CYP1A2 activity, (D) CYP2A6 activity, (E) CYP2C9 activity and (F) CYP3A4 activity. Arrows indicate undetectable data. $^{**}P < 0.01$ and $^{****}P < 0.0001$.

2.5 REFERENCES

[1] A. Sivaraman, J.K. Leach, S. Townsend, T. Iida, B.J. Hogan, D.B. Stolz, R. Fry, L.D. Samson, S.R. Tannenbaum, L.G. Griffith, A microscale in vitro physiological model of the liver: predictive screens for drug metabolism and enzyme induction, Curr Drug Metab 6(6) (2005) 569-91.

[2] M. Strazzabosco, C. Spirli, L. Okolicsanyi, Pathophysiology of the intrahepatic biliary epithelium, J Gastroenterol Hepatol 15(3) (2000) 244-53.

[3] G. Alpini, J.M. McGill, N.F. Larusso, The pathobiology of biliary epithelia, Hepatology 35(5) (2002) 1256-68.

[4] K.-S. Yoo, W.T. Lim, H.S. Choi, Biology of Cholangiocytes: From Bench to Bedside, Gut and Liver 10(5) (2016) 687-698.

[5] D. Alvaro, M.G. Mancino, S. Glaser, E. Gaudio, M. Marzioni, H. Francis, G. Alpini, Proliferating cholangiocytes: a neuroendocrine compartment in the diseased liver, Gastroenterology 132(1) (2007) 415-31.

[6] S.R. Khetani, S.N. Bhatia, Microscale culture of human liver cells for drug development, Nat Biotechnol 26(1) (2008) 120-6.

[7] B. Clement, C. Guguen-Guillouzo, J.P. Campion, D. Glaise, M. Bourel, A. Guillouzo, Long-term co-cultures of adult human hepatocytes with rat liver epithelial cells: modulation of albumin secretion and accumulation of extracellular material, Hepatology 4(3) (1984) 373-80.

[8] J.M. Caviglia, R.F. Schwabe, Mouse models of liver cancer, Methods Mol Biol 1267 (2015) 165-83.

[9] J. Seok, H.S. Warren, A.G. Cuenca, M.N. Mindrinos, H.V. Baker, W. Xu, D.R. Richards, G.P. McDonald-Smith, H. Gao, L. Hennessy, C.C. Finnerty, C.M. Lopez, S. Honari, E.E. Moore, J.P. Minei, J. Cuschieri, P.E. Bankey, J.L. Johnson, J. Sperry, A.B. Nathens, T.R. Billiar, M.A. West, M.G. Jeschke, M.B. Klein, R.L. Gamelli, N.S. Gibran, B.H. Brownstein, C. Miller-Graziano, S.E. Calvano, P.H. Mason, J.P. Cobb, L.G. Rahme, S.F. Lowry, R.V. Maier, L.L. Moldawer, D.N. Herndon, R.W. Davis, W. Xiao, R.G. Tompkins, Inflammation, L.S.C.R.P. Host Response to Injury, Genomic responses in mouse models poorly mimic human inflammatory diseases, Proc Natl Acad Sci U S A 110(9) (2013) 3507-12.

[10] S.F. Schlosser, A.D. Burgstahler, M.H. Nathanson, Isolated rat hepatocytes can signal to other hepatocytes and bile duct cells by release of nucleotides, Proc Natl Acad Sci U S A 93(18) (1996) 9948-53.

[11] A. Raven, W.Y. Lu, T.Y. Man, S. Ferreira-Gonzalez, E. O'Duibhir, B.J. Dwyer, J.P. Thomson, R.R. Meehan, R. Bogorad, V. Koteliansky, Y. Kotelevtsev, C. Ffrench-Constant, L.

Boulter, S.J. Forbes, Cholangiocytes act as facultative liver stem cells during impaired hepatocyte regeneration, Nature 547(7663) (2017) 350-354.

[12] M.D. Davidson, K.R. Ballinger, S.R. Khetani, Long-term exposure to abnormal glucose levels alters drug metabolism pathways and insulin sensitivity in primary human hepatocytes, Sci Rep 6 (2016) 28178.

[13] S.R. Khetani, D.R. Berger, K.R. Ballinger, M.D. Davidson, C. Lin, B.R. Ware, Microengineered liver tissues for drug testing, J Lab Autom 20(3) (2015) 216-50.

[14] M.D. Davidson, D.A. Kukla, S.R. Khetani, Microengineered cultures containing human hepatic stellate cells and hepatocytes for drug development, Integr Biol (Camb) 9(8) (2017) 662-677.

[15] U.E. Lee, S.L. Friedman, Mechanisms of hepatic fibrogenesis, Best Pract Res Clin Gastroenterol 25(2) (2011) 195-206.

[16] S.L. Friedman, Hepatic stellate cells: protean, multifunctional, and enigmatic cells of the liver, Physiol Rev 88(1) (2008) 125-72.

[17] R. Joplin, T. Hishida, H. Tsubouchi, Y. Daikuhara, R. Ayres, J.M. Neuberger, A.J. Strain, Human intrahepatic biliary epithelial cells proliferate in vitro in response to human hepatocyte growth factor, J Clin Invest 90(4) (1992) 1284-9.

[18] G. Lesage, S.S. Glaser, S. Gubba, W.E. Robertson, J.L. Phinizy, J. Lasater, R.E. Rodgers, G. Alpini, Regrowth of the rat biliary tree after 70% partial hepatectomy is coupled to increased secretin-induced ductal secretion, Gastroenterology 111(6) (1996) 1633-44.

[19] G.D. LeSage, A. Benedetti, S. Glaser, L. Marucci, Z. Tretjak, A. Caligiuri, R. Rodgers, J.L. Phinizy, L. Baiocchi, H. Francis, J. Lasater, L. Ugili, G. Alpini, Acute carbon tetrachloride feeding selectively damages large, but not small, cholangiocytes from normal rat liver, Hepatology 29(2) (1999) 307-19.

[20] R. Joplin, A.J. Strain, J.M. Neuberger, Biliary epithelial cells from the liver of patients with primary biliary cirrhosis: isolation, characterization, and short-term culture, J Pathol 162(3) (1990) 255-60.

[21] R. Joplin, A.J. Strain, J.M. Neuberger, Immuno-isolation and culture of biliary epithelial cells from normal human liver, In Vitro Cell Dev Biol 25(12) (1989) 1189-92.

[22] G. Alpini, S. Glaser, W. Robertson, J.L. Phinizy, R.E. Rodgers, A. Caligiuri, G. LeSage, Bile acids stimulate proliferative and secretory events in large but not small cholangiocytes, Am J Physiol 273(2 Pt 1) (1997) G518-29.

[23] D. Alvaro, P. Onori, V.D. Metalli, G. Svegliati-Baroni, F. Folli, A. Franchitto, G. Alpini, M.G. Mancino, A.F. Attili, E. Gaudio, Intracellular pathways mediating estrogen-induced cholangiocyte proliferation in the rat, Hepatology 36(2) (2002) 297-304.

[24] H. Francis, S. Glaser, Y. Ueno, G. Lesage, L. Marucci, A. Benedetti, S. Taffetani, M. Marzioni, D. Alvaro, J. Venter, R. Reichenbach, G. Fava, J.L. Phinizy, G. Alpini, cAMP stimulates the secretory and proliferative capacity of the rat intrahepatic biliary epithelium through changes in the PKA/Src/MEK/ERK1/2 pathway, J Hepatol 41(4) (2004) 528-37.

[25] A. Celli, F.G. Que, Dysregulation of apoptosis in the cholangiopathies and cholangiocarcinoma, Semin Liver Dis 18(2) (1998) 177-85.

[26] K.N. Lazaridis, M. Strazzabosco, N.F. Larusso, The cholangiopathies: disorders of biliary epithelia, Gastroenterology 127(5) (2004) 1565-77.

[27] J. Tinmouth, M. Lee, I.R. Wanless, F.W. Tsui, R. Inman, E.J. Heathcote, Apoptosis of biliary epithelial cells in primary biliary cirrhosis and primary sclerosing cholangitis, Liver 22(3) (2002) 228-34.

[28] M.M. Richardson, J.R. Jonsson, E.E. Powell, E.M. Brunt, B.A. Neuschwander-Tetri, P.S. Bhathal, J.B. Dixon, M.D. Weltman, H. Tilg, A.R. Moschen, D.M. Purdie, A.J. Demetris, A.D. Clouston, Progressive fibrosis in nonalcoholic steatohepatitis: association with altered regeneration and a ductular reaction, Gastroenterology 133(1) (2007) 80-90.

[29] M.B. Ray, C.L. Mendenhall, S.W. French, P.S. Gartside, Bile duct changes in alcoholic liver disease. The Veterans Administration Cooperative Study Group, Liver 13(1) (1993) 36-45.

[30] A.D. Clouston, E.E. Powell, M.J. Walsh, M.M. Richardson, A.J. Demetris, J.R. Jonsson, Fibrosis correlates with a ductular reaction in hepatitis C: roles of impaired replication, progenitor cells and steatosis, Hepatology 41(4) (2005) 809-18.

[31] T.M. De Assuncao, Y. Sun, N. Jalan-Sakrikar, M.C. Drinane, B.Q. Huang, Y. Li, J.I. Davila, R. Wang, S.P. O'Hara, G.A. Lomberk, R.A. Urrutia, Y. Ikeda, R.C. Huebert, Development and characterization of human-induced pluripotent stem cell-derived cholangiocytes, Lab Invest 95(10) (2015) 1218.

[32] L. Loarca, T.M. De Assuncao, N. Jalan-Sakrikar, S. Bronk, A. Krishnan, B. Huang, L. Morton, C. Trussoni, L.M. Bonilla, E. Krueger, S. O'Hara, P. Splinter, G. Shi, M.J.L. Pisarello, G.J. Gores, R.C. Huebert, N.F. LaRusso, Development and characterization of cholangioids from normal and diseased human cholangiocytes as an in vitro model to study primary sclerosing cholangitis, Lab Invest 97(11) (2017) 1385-1396.

[33] N.K. Van Hul, J. Abarca-Quinones, C. Sempoux, Y. Horsmans, I.A. Leclercq, Relation between liver progenitor cell expansion and extracellular matrix deposition in a CDE-induced murine model of chronic liver injury, Hepatology 49(5) (2009) 1625-35.

[34] M.N. Jhandier, E.A. Kruglov, E.G. Lavoie, J. Sevigny, J.A. Dranoff, Portal fibroblasts regulate the proliferation of bile duct epithelia via expression of NTPDase2, J Biol Chem 280(24) (2005) 22986-92.

[35] Y. He, G.D. Wu, T. Sadahiro, S.I. Noh, H. Wang, D. Talavera, H. Wang, J.M. Vierling, A.S. Klein, Interaction of CD44 and hyaluronic acid enhances biliary epithelial proliferation in cholestatic livers, Am J Physiol Gastrointest Liver Physiol 295(2) (2008) G305-12.

[36] S.J. Forbes, M. Parola, Liver fibrogenic cells, Best Pract Res Clin Gastroenterol 25(2) (2011) 207-17.

[37] J.A. Dranoff, R.G. Wells, Portal fibroblasts: Underappreciated mediators of biliary fibrosis, Hepatology 51(4) (2010) 1438-44.

[38] S. Lemoinne, A. Cadoret, H. El Mourabit, D. Thabut, C. Housset, Origins and functions of liver myofibroblasts, Biochim Biophys Acta 1832(7) (2013) 948-54.

[39] C. Degott, E.S. Zafrani, P. Callard, B. Balkau, R.E. Poupon, R. Poupon, Histopathological study of primary biliary cirrhosis and the effect of ursodeoxycholic acid treatment on histology progression, Hepatology 29(4) (1999) 1007-12.

[40] S. Michalak, M.C. Rousselet, P. Bedossa, C. Pilette, D. Chappard, F. Oberti, Y. Gallois, P. Cales, Respective roles of porto-septal fibrosis and centrilobular fibrosis in alcoholic liver disease, J Pathol 201(1) (2003) 55-62.

[41] V. Nobili, G. Carpino, A. Alisi, A. Franchitto, G. Alpini, R. De Vito, P. Onori, D. Alvaro, E. Gaudio, Hepatic progenitor cells activation, fibrosis, and adipokines production in pediatric nonalcoholic fatty liver disease, Hepatology 56(6) (2012) 2142-53.

[42] S.R. Khetani, Micropatterned co-cultures of hepatocytes and nonparenchymal cells : mechanisms of differentiation, dynamics and applications, (2006).

[43] B.R. Ware, M.J. Durham, C.P. Monckton, S.R. Khetani, A Cell Culture Platform to Maintain Long-term Phenotype of Primary Human Hepatocytes and Endothelial Cells, Cell Mol Gastroenterol Hepatol 5(3) (2018) 187-207.

[44] B.R. Ware, M.J. Durham, C.P. Monckton, S.R. Khetani, A Cell Culture Platform to Maintain Long-term Phenotype of Primary Human Hepatocytes and Endothelial Cells, Cellular and Molecular Gastroenterology and Hepatology (2017).

CHAPTER 3. VITA

NAME	Jennifer S. Liu
EDUCATION	M.S., Bioengineering, University of Illinois at Chicago, expected 2018
	B.S., Life Science, Fu Jen Catholic University, Taipei, Taiwan, 2011
WORKING	Research Assistant, Pathology Department of Taipei Medical University Hospital, Taipei, Taiwan, July, 2012 – February, 2015
	Intern, Graduate Institute of Basic Medicine, Fu Jen Catholic University, Taipei, Taiwan, July, 2009 – June, 2010